

# A Survey of Deep Face Restoration: Denoise, Super-Resolution, Deblur, Artifact Removal

Tao Wang, Kaihao Zhang, Xuanxi Chen, Wenhan Luo, Jiankang Deng,  
Tong Lu, Xiaochun Cao, Wei Liu, Hongdong Li, Stefanos Zafeiriou

**Abstract**—Face Restoration (FR) aims to restore High-Quality (HQ) faces from Low-Quality (LQ) input images, which is a domain-specific image restoration problem in the low-level computer vision area. The early face restoration methods mainly use statistic priors and degradation models, which are difficult to meet the requirements of real-world applications in practice. In recent years, face restoration has witnessed great progress after stepping into the deep learning era. However, there are few works to study deep learning-based face restoration methods systematically. Thus, this paper comprehensively surveys recent advances in deep learning techniques for face restoration. Specifically, we first summarize different problem formulations and analyze the characteristic of the face image. Second, we discuss the challenges of face restoration. Concerning these challenges, we present a comprehensive review of existing FR methods, including prior based methods and deep learning-based methods. Then, we explore developed techniques in the task of FR covering network architectures, loss functions, and benchmark datasets. We also conduct a systematic benchmark evaluation on representative methods. Finally, we discuss future directions, including network designs, metrics, benchmark datasets, applications, *etc.* We also provide an open-source repository for all the discussed methods, which is available at <https://github.com/TaoWangzj/Awesome-Face-Restoration>.

**Index Terms**—Face restoration, Deep learning, Survey, Low-level vision, Facial prior, Face deblurring, Face denoising, Face super-resolution, Face hallucination, Face artifact removal.



## 1 INTRODUCTION

FACE restoration, a domain-specific image restoration problem, is a classic task in the fields of image processing and computer vision. Face restoration is to restore the high-quality face image  $I_{hq}$  from the degraded face image  $I_{lq} = \mathcal{D}(I_{hq}) + n_{\delta}$ , where  $\mathcal{D}$  is the noise-irrelevant degradation function, and  $n_{\delta}$  is the additive noise. According to different forms of the degradation function  $\mathcal{D}$ , the face restoration task can be divided into five main categories: (1) **face denoising**, which refers to removing the noise (*e.g.*, Gaussian noise) contained in the face image [1], [2], (2) **face deblurring**, which is to recover a latent sharp face image from a blurry face image caused by various factors such as camera shake or object motion [3], [4], (3) **face super-resolution** (also known as face hallucination [5]), which aims to enhance quality and resolution of low-resolution facial images [6], [7], (4) **face artifact removal**, which refers to recovering high-quality face images from the given low-quality face images with artifacts caused by lossy compression in the process of image storage and transmission [8], [9], (5) **blind face restoration**, which aims at restoring high-quality face images from the low-quality ones without the knowledge of degradation

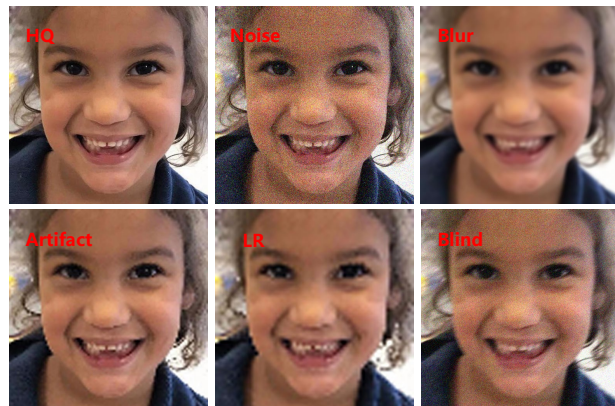


**Fig. 1:** Examples of low-quality face images degraded from high-quality (HQ) image, with respect to noise, blur, artifact, low resolution and mix of the above factors.

types or parameters [8], [9]. Fig. 1 illustrates exemplar low-quality face images caused by these forms of degradation, which influence not only the visual quality, but also the performance of downstream computer vision algorithms. Thus, face restoration has a wide range of applications, including face recognition [10], privacy protection [11], and autonomous driving [12].

Early face restoration methods mainly focus on statistic prior and degradation models, which can be approximately divided into Bayesian inference based methods [6], [13], subspace learning based methods [14], [15], sparse representation based methods [16], [17], *etc.* In recent years, deep learning-based methods have attracted more and more attention with the development of deep learning and the availability of large-scale datasets. Thus, a large number of deep learning-based methods for face restoration have been proposed in the literature. Generally speaking, deep learning-

- T. Wang, X. Chen and T. Lu are with the State Key Laboratory for Novel Software Technology, Nanjing University, Nanjing, 210023, China, (e-mail: taowangzj@gmail.com, xuanxichen.nju@gmail.com, lutong@nju.edu.cn).
- K. Zhang and H. Li are with the College of Engineering and Computer Science, Australian National University, Canberra, ACT, Australia, (e-mail: {super.khzhang, hongdong.li}@gmail.com).
- W. Luo and X. Cao are with Shenzhen Campus of Sun Yat-sen University, Shenzhen, 518107, China, (e-mail: whluo.china@gmail.com, caoxiaochun@mail.sysu.edu.cn).
- J. Deng and S. Zafeiriou are with Department of Computing, Imperial College London, London, UK, (e-mail: {j.deng16, s.zafeiriou}@imperial.ac.uk).
- W. Liu is with Tencent, Shenzhen, 518107, China, (e-mail: wi2223@columbia.edu).

Corresponding authors: W. Luo and T. Lu.

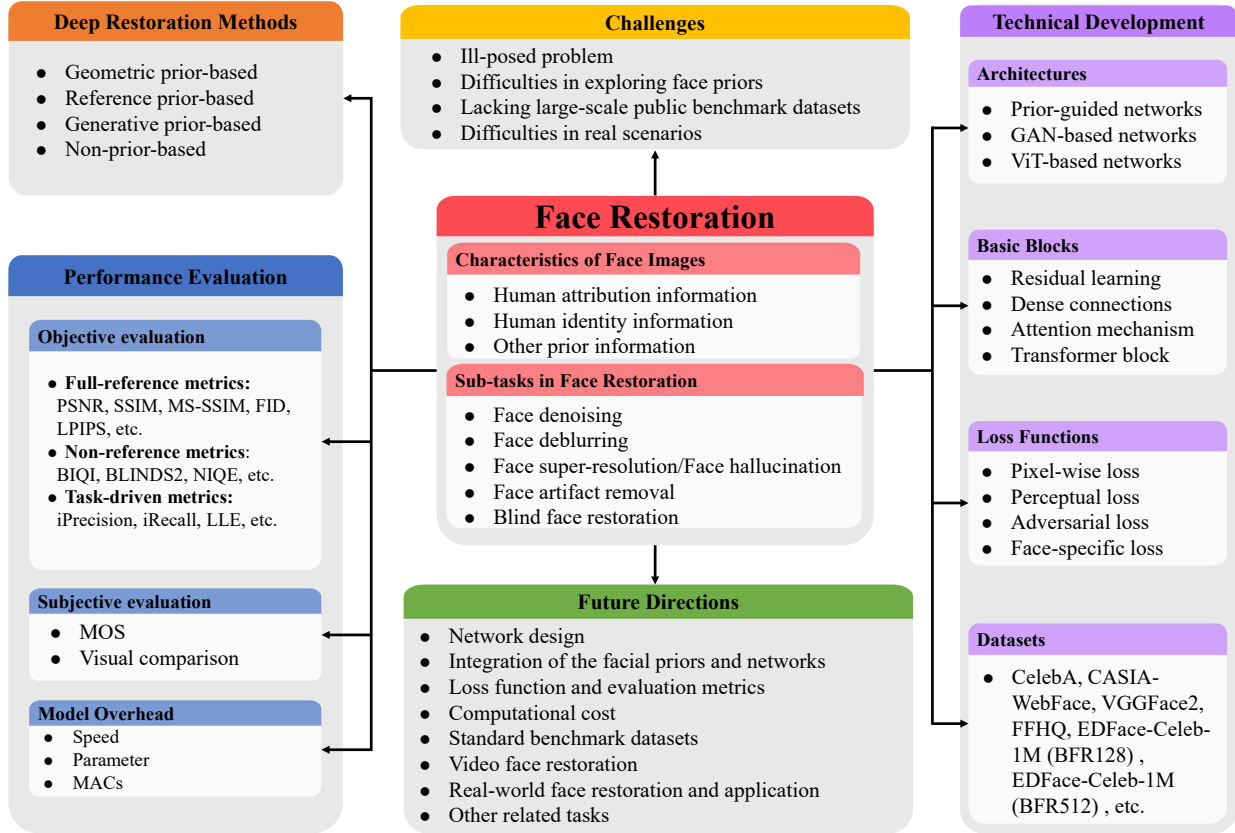


Fig. 2: Taxonomy of this survey on face restoration using deep learning techniques.

based face restoration methods adopt different techniques to build state-of-the-art networks. The employed techniques mainly focus on the following aspects: different deep learning architectures [7], [18], [19], [20], different facial priors [21], [22], [23], [24], different loss functions [21], [25], [26], [27], different learning strategies [28], [29], *etc.* Although deep learning solutions have dominated the research of face restoration in recent years, there is still a lack of in-depth and comprehensive surveys on face restoration with deep learning technology. Thus, this paper provides a comprehensive and systematic review of deep learning methods for the face restoration task.

### 1.1 Differences from Other Related Reviews

So far, there are few surveys about the overview of the face restoration task, though some surveys are related to the topic of face restoration, as shown in Table 1. We divide them into three groups and discuss their differences in the following. (1) The first group [30], [31], [32], [33], [34] aims to discuss general image restoration using deep learning techniques. For example, In [30], [31], [32], [33], they discuss the common causes of one specific task in image restoration such as deraining, denoising, super-resolution, and deblurring, respectively, and review different deep learning-based methods. [34] pays more attention to reviewing deep learning methods for general image restoration tasks that include image deblurring, denoising, dehazing, and super-resolution. (2) The second group [35], [36], [37], [38] focuses on reviewing the advances and development in traditional face super-resolution methods such as subspace learning based methods [14], [15], and sparse representation based methods [16], [17]. (3) The third group [39], [40] reviews the recent development in face super-resolution with deep learning techniques. Although the topic

TABLE 1: A summary of other literature reviews.

References	Related Topic	Year
Yang <i>et al.</i> [30]	Image Deraining Using Deep Learning	2020
Tian <i>et al.</i> [31]	Image denoising Using Deep Learning	2020
Wang <i>et al.</i> [32]	Image Super-Resolution Using Deep Learning	2020
Zhang <i>et al.</i> [33]	Image Deblurring Using Deep Learning	2022
Su <i>et al.</i> [34]	Image Restoration Using Deep Learning	2022
Liang <i>et al.</i> [35]	Face Super-Resolution Using Traditional Methods	2012
Wang <i>et al.</i> [36]		2014
Nguyen <i>et al.</i> [37]		2018
Rajput <i>et al.</i> [38]		2018
Liu <i>et al.</i> [39]	Face Super-Resolution Using GAN	2019
Jiang <i>et al.</i> [40]	Face Super-Resolution Using Deep Learning	2021

is related to ours, they focus only on the specific task of face super-resolution, whose scope is narrower than ours. Differently, our work systematically and comprehensively reviews recent advances in deep learning-based methods for face denoising, face deblurring, face super-resolution, face artifact removal, and blind face restoration tasks.

### 1.2 Our Contributions

This work systematically and comprehensively reviews the research progress of face restoration technology in recent years. The taxonomy of this survey is shown in Fig. 2. We conduct this survey in different aspects, including problem formulation, existing challenges, state-of-the-art methods, technical development, performance evaluation, and future directions. The contributions of this paper are summarized as follows. (I) We discuss the main degradation models in face restoration, the commonly used metrics, and the characteristic of face images that differ from natural images. (II) We discuss existing challenges in face restoration and provide a comprehensive overview of existing deep learning-based face restoration methods. (III) We provide in-depth analysis and discussion about the technical development of the methods,

covering network architecture, basic blocks, loss functions, and benchmark datasets. (IV) We conduct a benchmark study of representative methods on popular face benchmarks, which will facilitate future experimental comparisons. (V) We analyze the open challenges of the face restoration task and discuss its future directions to guide future research for the community.

### 1.3 Organization of This Review

The remainder of this paper is organized as follows. In Section 2, we successively introduce the problem definitions of five common face restoration tasks, the image quality evaluation metrics, and the characteristics of face images. In Section 3, we discuss the challenges of face restoration and analyze how existing face restoration methods address these challenges. Section 4 reviews the technical development of deep face restoration, including network architectures, basic blocks, loss functions, and datasets. Section 5 reports the experimental results of existing methods. In Section 6, we discuss the future directions of face restoration. Finally, Section 7 concludes this paper.

## 2 BACKGROUND

### 2.1 Problem Formulation

Image degradation occurs during image formation, transmission, and storage. The degradation may be in several forms for real-world facial images, including additive noise, space invariant or variant blur, aliasing, and compression artifact. In general, the face image degradation model can be formulated as:

$$I_{lq} = \mathcal{D}(I_{hq}; n_\delta), \quad (1)$$

where  $I_{lq}$  is the low-quality face image,  $\mathcal{D}$  refers to the noise-irrelevant degradation function,  $I_{hq}$  is the corresponding high-quality face image, and  $n$  usually denotes additive white Gaussian noise with a noise level  $\delta$ . By specifying different  $\mathcal{D}$ , one can get different degradation. For example, noise degradation [41], [42] that  $\mathcal{D}$  is an identity function. Blur degradation [33], [43] where  $\mathcal{D}$  is a convolution/averaging operation. Low-resolution degradation [44], [45], [46], [47] when  $\mathcal{D}$  is a combination of the convolution and downsampling operations. Artifact degradation [48], [49] when  $\mathcal{D}$  is a JPEG compression operation. Mixed degradation [8], [9] when  $\mathcal{D}$  is a combo of various factors.

FR refers to the recovery of a high-quality face image from its degraded low-quality counterpart. Namely, it aims to find the inverse of the degradation model in Eq. 1 as:

$$I_{hq} = \mathcal{D}^{-1}(I_{lq}; n_\delta), \quad (2)$$

where  $\mathcal{D}^{-1}$  is the face restoration model. If the degradation factors are provided, the FR task is regarded as non-blind face restoration, like face denoising, face deblurring, face super-resolution, and face artifact removal. Otherwise, the FR task is called blind face restoration. In the following, we detail the specific problem definition of sub-tasks in FR, where we mainly introduce some commonly used degradation models.

**Face Denoising.** This sub-task focuses on removing noise from an observed noisy face image. The noisy face image is typically constructed by the additive model, which is formulated as:

$$I_n = I_c + n_\delta, \quad (3)$$

where  $I_c$ ,  $I_n$  and  $n_\delta$  represent the clean face image, noisy face image, and additive Gaussian noise with a noise level  $\delta$ , respectively. Face Denoising is to find the inverse of the degradation model.

**Face Deblurring.** Face blur is a common problem in captured face images. It mainly contains motion blur [50] caused by the relative movement between the object and the camera, out-of-focus blur [51] caused by the misalignment between the target and the camera focus. Face deblurring mainly considers motion blur, which can be modeled as:

$$I_b = k_\sigma * I_s + n_\delta, \quad (4)$$

where  $I_b$  is the blurry face image,  $I_s$  is the sharp face image,  $k_\sigma$  is the blur kernel,  $*$  is the convolution operation, and  $n_\delta$  is the additive noise. Face deblurring is to obtain the inverse function of the degradation model, so as to generate sharp face images.

**Face Super-Resolution.** As a domain-specific image super-resolution problem, face Super-resolution refers to enhancing the resolution of low-resolution (LR) face images and producing high-resolution (HR) face images with rich details. The degradation model is formulated as:

$$I_{lr} = (I_{hr} * k_\sigma) \downarrow_s + n_\delta, \quad (5)$$

where  $I_{lr}$  is the low-resolution face image,  $I_{hr}$  is the high-resolution face image,  $k_\sigma$  is the blur kernel,  $*$  is the convolutional operation,  $n_\delta$  is the noise, and  $\downarrow_s$  is the downsampling operation with a scale factor  $s$ .  $s$  is usually set as 2, 3, 4, and 8 in the face super-resolution task. Based on the degradation, face super-resolution aims to simulate the inverse process of the degradation model and recover the HR face image from the LR face image.

**Face Artifact Removal.** In real-world applications, lossy compression techniques (e.g., JPEG, Webp, and HEVC-MSP) are widely adopted for saving storage space and bandwidth. However, lossy compression easily leads to information loss and introduces undesired artifacts for recorded face images. Given a high-quality face image  $I_{hq}$ , its compression process is as follows:

$$I_{lq} = J(I_{hq}) + n_\delta, \quad (6)$$

where  $I_{lq}$  is the compressed face image,  $J$  denotes the image compression. As JPEG is the most extensively used way for image compression, researchers thus focus more on this type of degradation in the task of face artifact removal. According to the image compression process, face artifact removal is devoted to learning the inverse process of the degradation model and generating the HQ face images.

**Blind Face Restoration.** Unlike focusing on a single type of degradation, blind face restoration aims to handle severely degraded face images in the wild. The degradation of face images is complex in this task, which is a random combination of noise, blur, low resolution, and JPEG compression artifacts. The degradation model of blind face restoration can be defined as:

$$I_{lq} = \{JPEG_q((I_{hq} * k_\sigma) \downarrow_s + n_\delta)\} \uparrow_s, \quad (7)$$

where  $*$  is the convolution operation,  $k_\sigma$  is the blur kernel,  $JPEG_q$  is JPEG compression function with quality factor  $q$ ,  $\downarrow_s$  is downsampling operation with scaling factor  $s$ ,  $n_\delta$  is the noise, and  $\uparrow_s$  is upsampling operation with scaling factor  $s$ . The goal of blind face restoration is to recover HQ face images by modeling the inverse process of the above degradation model.

### 2.2 Image Quality Assessment

It is important to assess the quality of the recovered images accurately. In general, image quality assessment can be approximately divided into two categories: subjective evaluation and objective

evaluation. The subject evaluation methods are related to the judgement of humans. A representative metric is Mean Opinion Score (MOS) [52], where human raters are invited to assign visual scores to the observed images. However, this kind of method is expensive and time-consuming. Thus, objective evaluation has been taken into consideration. In the face restoration task, the objective evaluation metrics can be broadly divided into full-reference, no-reference, and task-driven metrics.

Full-reference metrics mainly work on measuring the difference between the recovered face image and its corresponding ground-truth image to assess the image quality. Typical full-reference metrics used in the FR task are PSNR [53], SSIM [54], MS-SSIM [55], FID [56] and LPIPS [57]. PSNR focuses more on the difference between each pixel from two images. Compared with PSNR, SSIM considers the image’s luminance, contrast, and structure when measuring the similarity. Based on SSIM, the MS-SSIM metric is proposed. It firstly divides the image into multiple windows, then calculates the SSIM of each window, and averages these SSIM values to acquire MS-SSIM. In contrast to PSNR, SSIM, and MS-SSIM, FID and LPIPS can assess the visual quality of face images. In contrast to pixel-wise metrics (PSNR, SSIM, and MS-SSIM), which prefer smooth results and are not consistent with human perception, FID and LPIPS are proposed to evaluate the perceptual realism of restored images.

Compared with Full-reference metrics, which rely on ground-truth images, no-reference metrics can directly assess image quality by only the recovered images. Many no-reference metrics can be used in FR, such as BIQI [58], BLINDS2 [59], BRISQUE [60], CORNIA [61], DIIVINE [62], NIQE [63] and SSEQ [64]. Among them, the NIQE metric is widely adopted in the literature [9], [19], [65] to measure the naturalness of real face image restoration results.

In addition, as a domain-specific image restoration task, a lot of task-driven metrics have been used, such as iPrecision [66], iRecall [66], LLE [8], Deg [9], AFLD [65] and AFICS [65]. These task-driven metrics are related to identity information in the face images, such as face landmark or face ID to evaluate the quality of face images.

### 2.3 Analysis of Face Image

As we can see, the captured face images contain a wide variety of information related to humans, such as human face geometry spatial distribution information. Thus, different from general image restoration task, the face geometry information (*i.e.*, facial prior) can be exploited for face restoration. In the past decades, a large amount of human face information in face images has been explored to assist in face restoration. Generally speaking, the information in face image can be divided into three categories: human attribute information, human identity information, and other prior information. We introduce them as follows.

**Human Attribute Information.** As illustrated in Fig. 3, a face image usually contains special attributes of a figure, such as gender, age, glasses, emotion *etc.* These face affiliated attributes are beneficial to multiple tasks, including face recognition [68], [69], face verification [70], and face restoration [71], [72]. As the degradation in face images is rather diverse and complex, it is difficult for the restoration model to recover the clear image relying only on the degraded image. Therefore, some methods [9], [71], [73] exploit human attributes in the face image as additional information to guide the restoration process. For example, Liu *et al.*

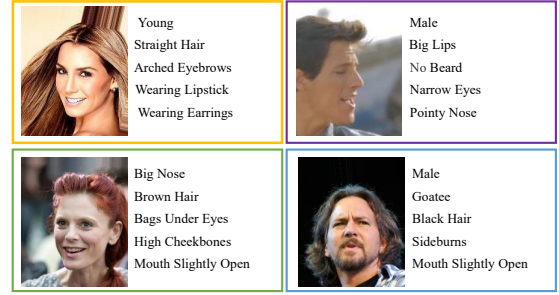


**Fig. 3:** Illustration of typical attributes in face images. The text on the right of each image describes the attributes of the face. The face images and their corresponding attributes are from the CelebA dataset [67].

[71] introduce the class-attribute information into the local detail restoration stage to further enhance local details.

**Human Identity Information.** In addition to the basic attributes in the face image, each face has its unique identity information. The identity information can be used for guiding the model to generate faces close to the real identity. On the one hand, human’s accurate perception of the face mainly depends on the identity information of the face. On the other hand, adopting only the pixel-level loss to supervise the restoration model training cannot produce accurate identity-related facial detail for the task of face restoration. For example, [28] can generate face images with high perceptual quality. However, it can not retain the face identity well in the recovered images. Thus, the identity information is introduced to improve both the recognizability and performance of face restoration in the literature [74], [75], [76].

**Other Prior Information.** As illustrated in Fig. 4, some representative facial priors in face restoration are facial landmarks [21], [77], facial heatmaps [24], facial parsing maps [78], and 3D face prior [79]. 1) Facial landmarks. They are some important reference points of facial components, such as eye centers, nose tips, and mouth corners of humans in the image. Different datasets provide different numbers of facial landmarks for each face image. For instance, CelebA dataset contains 5 landmarks [67], FFHQ dataset includes 68 landmarks [80], and Helen dataset provides 194 landmarks [81]. In addition, various facial landmark detection methods [82], [83] can help detect landmarks. 2) Facial heatmaps. Compared to facial landmarks directly providing reference points of facial components, facial heatmaps describe the probability that reference points being facial landmarks. Specifically, based on the facial landmarks, each landmark is encoded by using a 2D Gaussian centered at the coordinates of that landmark to generate the facial heatmaps. 3) Facial parsing maps. These are semantic feature maps of face images, which are separated out face components (*e.g.*, nose, skin, eyes, and hair) from the face images. 4) 3D face prior. In contrast to the 2D prior without considering high dimensional information (*e.g.*, position and shape of faces), 3D face prior is developed for face restoration [79]. 3D face prior provides rich 3D knowledge based on the fusion of different face attributes (*e.g.*, identity, facial expression, illumination, and face pose). In addition, reference based prior [22], [29] and generative prior [9], [23] are introduced in the literature to guide the face restoration models.

## 3 LITERATURE SURVEY

In this section, we first briefly analyze the challenges in face restoration tasks. Then, we present a systematic overview of face image restoration methods, including prior based deep restoration methods and non-prior based deep restoration methods.

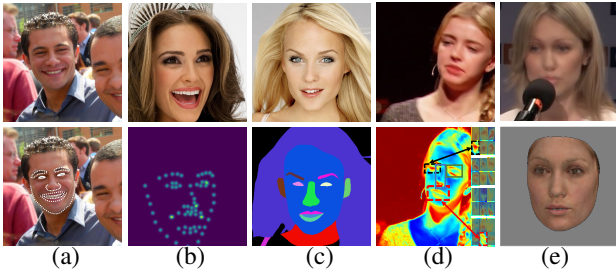


**Fig. 4:** Illustration of popular face priors contained in face images. The top row shows face images, and the bottom row shows corresponding priors. (a) Facial landmarks [21], [77], (b) Facial heatmaps [24], (c) Facial parsing map [78], (d) Facial dictionary [29], (e) 3D face prior [79].

### 3.1 Face Restoration Challenges

As a domain-specific image restoration task, face restoration aims to remove various unknown degradation in the low-quality face image and construct a high-quality one. However, there are several challenges in the task of face restoration.

**Ill-posed problem.** Although most existing methods are specifically developed for dealing with one single face restoration task, it is still an ill-posed problem, as the degradation types and degradation parameters of low-quality face images are unknown in advance. On the other hand, in practical scenarios, the degradation of face images is complex and diverse. Thus how to design effective and robust face restoration models to restore clear face images is a challenging problem.

**Difficulties in exploring face priors.** As a domain-specific image restoration task, some facial priors can be explored for face image restoration. Typical facial priors used in the literature include 1D vectors (identity and attributes), 2D images (facial landmarks, facial heatmaps, and facial parsing maps), and 3D prior. However, it is difficult to exploit the prior knowledge, because facial priors such as facial components and facial landmarks are usually extracted or estimated from low-quality images, which may be inaccurate and therefore directly affect the restoration performance. On the other hand, real-world low-quality images often contain complex and diverse degradation, and it is difficult to find appropriate priors to assist the process of face restoration. In addition, face restoration is different from image restoration due to the speciality of face images. For example, human eyes are more sensitive to face artifacts, bearing in mind with strong expectation of human face structure. Thus it brings another difficulty in restoring the human face.

**Lacking large-scale public benchmark datasets.** With the development of deep learning techniques, deep learning-based methods have shown impressive performance in face restoration. Most deep learning-based face restoration methods strongly rely on large-scale datasets to train networks. However, most of the current face restoration methods are trained or tested on non-public datasets. Especially in their experiments, these methods usually synthesize low-quality images using their private schemes based on the high-quality images and randomly split them for training and evaluation respectively [7], [27], [84]. Though some works use fixed training/testing sets [8], [9], [23], [29], the synthesized low-quality images are still different due to random noise, random combinations of degradation factors, *etc.* Therefore, it is still difficult to directly compare existing methods based on the reported results. Lacking public datasets directly leads to unfair performance comparison. In addition, lacking high-quality and large-scale benchmarks limits the potential of models. Therefore, it is a challenge to build more

proper benchmark datasets for face restoration.

**Difficulties in real-world scenarios.** Though deep learning methods have acquired state-of-the-art performance in face restoration, most of them work in a supervised manner. Specifically, these approaches require a paired (low-quality and high-quality image pair) dataset, and they would fail if the conditions are unsatisfied. However, it is difficult to collect large-scale datasets with real paired samples in the real world due to the complex and changeable scene. Therefore, most methods synthesize low-quality images by degradation models to approximate the real low-quality image. In addition, the synthesized low-quality face images are probably less informative and inconsistent with real-world images. The models trained on synthetic data sets can easily lead to domain drift, which limits the applicability of the model in real scenarios.

In the following, we will introduce and analyze in detail how existing face restoration methods deal with the above challenges.

### 3.2 Face Restoration Methods

General image restoration methods aim to design efficient methods for recovering sharp natural images. However, as a highly structured object, the human face has specific characteristics that are ignored by general image restoration methods. Thus, most face restoration methods incorporate face prior knowledge to recover facial images with clearer facial structure. The developed face-specific priors in the models are mainly based on common sense that human faces exhibit small variations in a controlled environment. On the other hand, other methods aim to develop networks learning a mapping function between the low-quality and high-quality face images without facial prior. The milestones of face restoration in the past years are illustrated in Fig. 5. We divide face restoration methods into two categories: prior based deep restoration methods and non-prior based deep learning approaches. In addition, prior based deep restoration methods can be approximately divided into three sets: geometric prior based deep restoration methods, reference prior based deep restoration methods, and generative prior based deep restoration methods. A summary of face restoration methods is shown in Table 2. In the following, we discuss these methods in detail.

#### 3.2.1 Geometric Prior Based Deep Restoration Methods

These methods mainly adopt the unique geometry and spatial distribution information of faces in the image to help the model progressively restore high-quality face images. Typical geometric priors include facial landmarks [21], [77], facial heatmaps [24] and facial parsing maps [78]. Chen *et al.* [21] make the first attempt to design the specific face geometric prior estimation sub-network in a deep network and train them in an end-to-end manner for the face super-resolution task. Specifically, they first use a coarse network to recover the coarse high-resolution image. Then the coarse image is sent to a fine super-resolution network and a prior information estimation network to extract image features and estimate landmark heatmaps and parsing maps respectively. In the end, both image features and geometric prior are fed to a fine super-resolution decoder to restore high-resolution images. This pioneering work improves the performance of face super-resolution while also providing a solution to estimating geometric prior directly from low-quality face images. Another representative work is Super-FAN proposed by Bulat and Tzimiropoulos [85]. Super-FAN is the first end-to-end system to simultaneously achieve facial super-resolution and facial landmark localization. The core

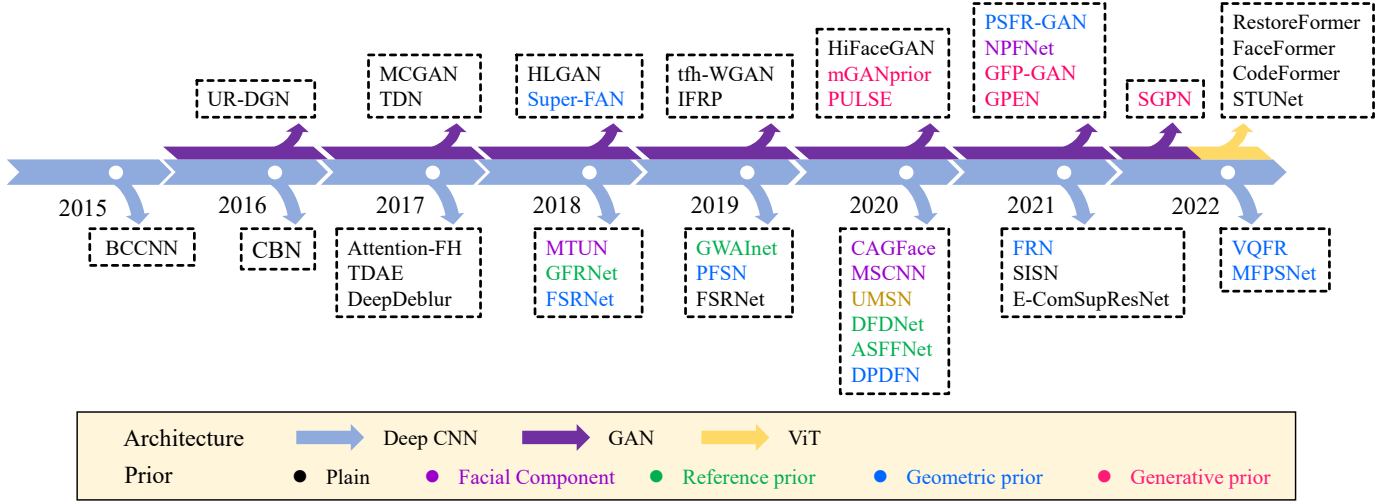


**Fig. 5:** Milestones of deep learning-based face restoration methods. We summarize the methods by different network architectures and facial priors. We list their names in the figure, and their details are shown in Table 2.

insight in Super-FAN is using the joint training strategy to guide the network to learn more face geometric information, which is achieved by integrating a face-alignment sub-network via heatmap regression and loss optimization. To further utilize facial attributes around the landmark for restoring facial details, Kim *et al.* [77] propose a lightweight face alignment network to generate facial landmark heatmaps for the face super-resolution network by a progressive training method. Some methods also resort to semantic information of the face. For example, Chen *et al.* [78] propose a multi-scale progressive model for face restoration, which recovers low-quality face images in a coarse-to-fine manner by semantic aware style transformation.

Compared with accurately estimating face landmarks or semantic maps directly from low-quality images, it is easy to localize facial components (not landmarks). Thus, another line of geometric prior based methods [3], [4], [24], [86], [87] is to take advantage of features of the facial component in human faces, *e.g.*, eyes and nose, as the prior information. Typically, MTUN [24] is one representative method that contains two branches. The first branch is used to super-resolve face images. The second branch is designed for estimating facial component heatmaps, where four heatmaps are employed to represent four components (*i.e.*, eyes, nose, mouth, and chin) of a human face. MTUN shows that utilizing information of facial components in low-quality face images can further improve the performance of face restoration. Recently, Yu *et al.* [88] make the first attempt to take full advantage of multi-geometric priors (*i.e.*, semantic-level parsing maps, geometric-level facial heatmaps, reference-level facial dictionaries, and pixel-level degraded image information) in the proposed network to guide face restoration. In contrast to the previously mentioned methods that focus on using 2D priors, Hu *et al.* [79] make the first attempt to embed 3D priors into networks for general face recovery tasks. Compared with 2D priors, 3D priors can integrate parameter descriptions of face attributes (*e.g.*, identity, facial expression, texture, illumination, and facial pose) to provide 3D morphological knowledge and further improve the face restoration performance.

### 3.2.2 Reference Prior Based Deep Restoration Methods

Previous works exploit facial prior purely relying on one single degraded image. It is worth noting that the degradation process generally is highly ill-posed, which fails to obtain accurate facial prior. Thus, several methods aim to guide the face restoration pro-

cess by using the facial structure or facial component dictionaries obtained from additional high-quality face images as reference prior [22], [26], [29], [73]. Some reference prior based methods utilize the additional information provided by a high-resolution guiding image with the same identity. Li *et al.* [22] and Dogan *et al.* [73] mainly employ a fixed frontal high-quality reference for each identity to provide additional identity-aware information to help the process of face restoration. Specifically, Li *et al.* propose a guided face restoration network (GFRNet) model consisting of a warping sub network (WarpNet) and a reconstruction sub network (RecNet) for face restoration. The WarpNet provides warped guidance, which aims to generate the flow field for warping the reference image to correct the pose and expression of the face. The RecNet takes both the low-quality image and warped guidance as input to recover the high-quality face image. In addition, due to the unavailability of the ground-truth flow field, they introduce a landmark loss to train WarpNet. Based on GFRNet, Dogan *et al.* [73] propose a GWAInet for face super-resolution, which is trained in an adversarial generative manner to generate high-quality face image. Compared with GFRNet, GWAInet does not rely on facial landmarks in the training stage, which guides the model to focus more on the whole face region and increases the robustness of the model. These two methods use a WarpNet to predict the flow field to warp the reference to align with the low-quality images. However, the alignment still does not solve all the differences between the reference and low-quality images, *i.e.*, mouth close to open. However, these two methods rely on a high-quality reference image with the same identity, which makes them only applicable in limited scenes. Thus, Li *et al.* [29] propose a deep face dictionary network (DFDNet) for face restoration, which uses deep component dictionaries as the reference prior to benefit the restoration process. In DFDNet, Li *et al.* first adopt K-means to produce facial component dictionaries for perceptually significant face components (*i.e.*, left/right eyes, nose, and mouth) from high-quality images. Then, they choose the most similar component features from generated component dictionaries to transfer the details to the low-quality face image and guide the model for face restoration.

### 3.2.3 Generative Prior Based Deep Restoration Methods

With the rapid development of generative adversarial network (GAN) [80], [103], recent works find that [23], [28] the generative

**TABLE 2:** An overview of face restoration methods using deep learning techniques. FSR is face super-resolution, FDB is face deblurring, and BFR is blind face restoration, including FSR, FDB, face denoising (FDN), face artifact removal (FAR), etc.

Methods	Prior	Architecture	Task	Key ideas	Publication	
BCCNN	Plain	Deep CNN	FSR	A <b>Bi-channel CNN</b> is proposed for face super restoration, which fuses the raw input and the face representations extracted from the deep CNN.	Zhou <i>et al.</i> 2015 [7]	
CBN			FSR	This work jointly optimizes <b>FSR and dense correspondence field estimation</b> in a deep bi-network, which benefits each other and recover high-quality face images.	Zhu <i>et al.</i> 2016 [89]	
Attention-FH			FSR	An Attention-aware network is developed. It aims to exploit the correlation cues from different facial parts by <b>attention mechanism</b> .	Cao <i>et al.</i> 2017 [84]	
TDAE			FSR	A <b>transformative autoencoder network</b> is proposed to super-resolve unaligned and tiny low-resolution face images. The network leverages a <b>decoder-encoder-decoder architecture</b> .	Yu and Porikli. 2017 [20]	
DeepDeblur			FDB	An <b>end-to-end CNN</b> is proposed for face deblurring. It is optimized with a <b>smoothness regularization</b> to keep facial identity information in the restored faces.	Wang <i>et al.</i> 2017 [27]	
E-ComSupResNet			FSR	This work designs an E-ComSupResNet network with the channel attention to super-resolve low resolution face images.	Chudasama <i>et al.</i> 2021 [90]	
SISN			FSR	This work proposes a SISN network with external-internal split attention group blocks. This attention block contains two paths designed for facial structure information and facial texture details.	Lu <i>et al.</i> 2021 [91]	
MTUN	Facial Component	Deep CNN	FSR	The work adopts <b>facial component heatmaps</b> to guide the upsampling stream in the network, which can help the network produce super-resolved faces with higher-quality details.	Yu <i>et al.</i> 2018 [24]	
CAGFace			FSR	A segmentation network is employed to generate <b>facial component-wise attention maps</b> to guide the model focus on face-inherent patterns.	Kalarot <i>et al.</i> 2020 [86]	
MSCNN			FDB	A multi-scale CNN is proposed to <b>exploit semantic prior and local structural constraints</b> for FDB.	Shen <i>et al.</i> 2020 [3]	
UMSN	Reference prior	Deep CNN	FDB	An uncertainty guided multi-stream semantic network is built for <b>exploiting face semantic information</b> for FDB.	Yasarla <i>et al.</i> 2020 [4]	
GFRNet			BFR	A guided face restoration model is proposed. It takes the degraded observation and a <b>high-quality guided image</b> from the same identity as input.	Li <i>et al.</i> 2018 [22]	
GWAInet			FSR	The proposed network aims to solve super-resolution on face images by <b>utilizing other high-resolution face images</b> of the same person.	Dogan <i>et al.</i> 2019 [73]	
DFDNet			BFR	The work uses K-means to <b>produce dictionaries</b> for face components in reference images and transfers the high-quality details into the degraded image for FR.	Li <i>et al.</i> 2020 [29]	
ASFFNet			BFR	This method enhances face restoration performance by utilizing <b>multi-exemplar images and adaptive feature fusion technique</b> .	Li <i>et al.</i> 2020 [26]	
FSRNet			BFR	This work proposes a multi-scale progressive network utilizing semantic information ( <b>face parsing maps</b> ).	Chen <i>et al.</i> 2018 [21]	
PFSN			FSR	A method combines a progressive training strategy, a compressed face alignment network, and a facial attention loss. The loss guides the network focus on <b>facial landmarks</b> .	Kim <i>et al.</i> 2019 [77]	
DPDFN	Geometric prior	Deep CNN	FSR	A <b>dual-path deep fusion network</b> is proposed for FSR without face prior. The network contains two individual branches, which are used to learn <b>global facial shape and local facial components</b> .	Jiang <i>et al.</i> 2020 [92]	
FRN			BFR	A <b>3D facial prior</b> is introduced into the model for face restoration. The estimated 3D facial prior provides spatial information of facial components and 3D visibility information.	Hu <i>et al.</i> 2021 [79]	
VQFR			FSR	The work proposes a <b>vector quantization based method</b> for FSR. It uses <b>high-quality feature banks</b> extracted from high-quality faces as a <b>dictionary</b> to guide the model to recover realistic facial detail.	Gu <i>et al.</i> 2022 [93]	
MFPSNet	BFR	MFPSNet employs typical facial priors ( <i>i.e.</i> , <b>facial parsing map, facial heatmaps and facial dictionary</b> ) to help the network restore high-quality face images.	Yu <i>et al.</i> 2022 [88]			
UR-DGN	Plain	GAN	FSR	A <b>GAN model</b> is proposed to learn an <b>end-to-end mapping</b> from low resolution to high resolution face images. And one <b>L2 regularization term</b> is used to guide the network to produce realistic images.	Yu and Porikli. 2016 [18]	
MCGAN			FSR	This work proposes a <b>multi-class GAN model</b> that can super-resolve both text and face images in a single generator network. It also introduces a <b>feature matching loss</b> to restore fine facial details.	Xu <i>et al.</i> 2017 [94]	
TDN			FSR	An <b>end-to-end GAN</b> is proposed to process unaligned and low-resolution faces for FSR. It aims to learn how to align and upsample face images by <b>exploiting the class specific information</b> .	Yu and Porikli. 2017 [95]	
HLGAN			FSR	A <b>two-stage method</b> is proposed. It designs a <b>High-to-Low GAN</b> to learn how to downgrade face images and then uses the output of this network to train a <b>Low-to-High GAN</b> for FSR.	Bulat <i>et al.</i> 2018 [96]	
tfh-WGAN			FSR	This work proposes a WGAN-based method. The core ideas are using auto encoding-based generator with both residual and concat-based skip connections.	Shao <i>et al.</i> 2019 [97]	
IFRP			BFR	This work develops an Identity-preserving Face Recovery from Portraits method. The generator is an auto encoder with residual block-embedded skip connections.	Shiri <i>et al.</i> 2019 [98]	
HiFaceGAN			BFR	This work views FR as a <b>semantic-guided generation problem</b> . It proposes a <b>multi-stage GAN network</b> with several collaborative suppression and replenishment units to generate high-quality faces.	Yang <i>et al.</i> 2020 [8]	
Super-FAN			Geometric prior	FSR	The network incorporates <b>facial structural information</b> in the architecture: a sub-network for face alignment and a face heatmap loss for optimization.	Bulat and Tzimiropoulos. 2018 [85]
PSFR-GAN				BFR	This work proposes a multi-scale progressive network utilizing semantic information ( <b>face parsing maps</b> ).	Chen <i>et al.</i> 2021 [78]
NPFNet			Facial Component	FSR	A progressive network with non-parametric facial prior enhancement is proposed to <b>extract and highlight facial components</b> for FSR.	Kim <i>et al.</i> 2021 [87]
mGANprior	Generative prior	BFR	An effective GAN method adopts <b>multiple GAN prior</b> and adaptive channel importance to recover clear face images.	Gu <i>et al.</i> 2020 [23]		
PULSE		FSR	The method <b>explores the latent space in GAN</b> to find regions that map to realistic images and down-scale correctly for FSR.	Menon <i>et al.</i> 2020 [28]		
GFP-GAN		BFR	The work incorporates the <b>generative facial prior</b> into the face restoration process of the deep network by spatial feature transform layers for BFR.	Wang <i>et al.</i> 2021 [9]		
GPEN		BFR	The method introduces a <b>pre-trained GAN</b> into a U-shaped deep neural network and fine-tunes the overall model for BFR.	Yang <i>et al.</i> 2021 [99]		
SGPN		BFR	This method integrates the <b>face sharp and generative prior</b> in the network for BFR.	Zhu <i>et al.</i> 2022 [100]		
RestoreFormer	Plain	ViT	BFR	A transformer network is proposed for face restoration. <b>The multi-head cross-attention layer</b> is designed to learn the spatial relationship between corrupted queries and high-quality key-value pairs.	Wang <i>et al.</i> 2022 [19]	
FaceFormer			BFR	A <b>scale-aware Transformer network</b> with the facial feature up-sampling module and facial feature embedding module is built to generate high-quality faces in the real-world scenarios.	Li <i>et al.</i> 2022 [101]	
CodeFormer			BFR	This work views the blind face restoration as a code prediction task. A <b>Transformer-based network</b> is proposed to model global components and context information from the low-quality faces for code prediction.	Zhou <i>et al.</i> 2022 [102]	
STUNet			BFR	A <b>Swin Transformer U-Net</b> is built to predict high-quality face images. This network mainly uses the <b>attention mechanism</b> and a <b>shifted window scheme</b> technique to capture important facial features.	Zhang <i>et al.</i> 2022 [65]	

prior of pre-trained face GAN models, such as StyleGAN [80], and StyleGAN2 [103], can provide rich and diverse facial information (e.g., geometry and facial textures). And researchers have started to leverage the GAN prior into face image restoration. The first kind of generative prior based methods is inspired by GAN inversion methods, which mainly aim at finding the closest latent vector in the GAN span from the input image. PULSE [28] is one representative method, which is a self-supervised face restoration method by optimizing the latent of a pre-trained StyleGAN [80]. Inspired by PULSE, mGANprior [23] considers multiple latent codes in the pre-trained GAN and optimizes multiple codes to promote the ability of image reconstruction. However, these methods fail to preserve fidelity in the restored face images. To achieve a better balance between visual quality and fidelity of the recovered images, recent works GFP-GAN [9] and GPEN [99] first extract fidelity information from the input low-quality face images and then leverage the pre-trained GAN as a decoder to capture facial prior. Specifically, GFP-GAN [9] leverages the facial distribution captured by a pre-trained GAN as facial prior to achieve joint restoration and color enhancement. GFP-GAN contains a degradation removal module and a pre-trained face GAN as facial prior. These two modules are bridged by a latent code mapping and several Channel-Split Spatial Feature Transform layers, which can achieve a good balance of realness and fidelity. GPEN [99] aims to effectively integrate the advantages of GAN and DNN for face restoration. In GPEN, they first learn a GAN used for generating high-quality face images and embed this pre-trained GAN into a deep neural network as a decoder prior for face restoration. More recently, Zhu *et al.* [100] propose to combine shape and generative prior to guide the process of face restoration for the network. In the proposed network, they first use a shape restoration module to generate shape prior. Then, a shape and generative prior integration module is proposed to fuse the shape and generative prior. Finally, they introduce a hybrid-level loss to jointly optimize the shape and generative prior with other network parts, and thus these two priors can better benefit the face restoration.

### 3.2.4 Non-prior Based Deep Restoration Methods

Although most deep learning-based FR methods can recover satisfying faces with the help of facial prior, it makes the cost of generating face images expensive and laborious. To address this problem, many methods aim to design a network that directly learns the mapping function between low-quality and high-quality face images without any additional facial priors. Some techniques are introduced in the models to improve the feature representation, such as multi-path structure, attention mechanism, feature fusion strategy, adversarial learning, strong backbone *etc.*

The first representative work is dated back to 2015. Zhou *et al.* [7] propose a bi-channel convolutional neural network (BCCNN) for face super-resolution. It consists of a feature extractor and an image generator. The proposed feature extractor extracts robust face representations from the low-resolution face image. The image generator is designed to adaptively fuse the extracted face representations and the input face image to generate the high-resolution image. BCCNN can achieve better restoration results for the face image with large variations. However, this work directly ignores pre-aligned facial spatial configurations (such as facial landmark localization) and, thus does not perform well when the input image has severe blur. To address this problem, Zhu *et al.* [89] propose a cascade bi-network called CBN to jointly optimize facial dense correspondence field estimation and face

super-resolution. CBN obtains better performance results than previous works. However, when the face feature location in the model is wrong, CBN may generate ghosting face images.

Following previous works [7], [89], some state-of-the-art methods [20], [27], [84], [92] focus on designing different CNN networks and learning strategies to improve the performance of the network. Among them, [92] is a representative work that aims at using recurrent and multi-path structures in the network to improve performance. Jiang *et al.* [92] propose a dual-path deep fusion network (DPDFN) for face super-resolution. The core insight of DPDFN is local and global feature learning and fusion in two branches. Over the past few years, GAN [104] has become another popular technology in the computer vision community. It has been widely applied in many applications, including image synthesis, semantic image editing, style transfer, classification, and image restoration. Compared with CNN, GAN can generate more realistic images [105]. The typical GAN structure consists of a generator network and a discriminator network. The generator is designed to produce realistic images, and the discriminator is used to figure out the difference between the image produced by the generator and the real image. The generator and discriminator are trained at the same time and compete against each other. In 2016, Yu and Porikli [18] make the first attempt to develop GAN and propose ultra-resolution by discriminative generative networks (UR-DGN) for face restoration. In UR-DGN, through an adversarial learning strategy, the discriminant network is used to learn the important components of human faces, and the generation network fuses these facial components into the input image. Following Yu and Porikli [18], many GAN based face restoration methods are proposed in the literature [8], [94], [95], [96], [97], [98]. These methods integrate many techniques (e.g., loss functions, learning strategies, identity constraints *etc.*) into the GAN network and achieve better visual results. Specifically, MCGAN [94] uses a multi-class GAN model and a feature matching loss. TDN [95] aims to exploit the class specific information in the process of restoration. HLGAN [96], tfh-WGAN [97], and HiFaceGAN [8] focus on designing more complex GAN models, including two-stage GANs, WGAN, and multi-stage GAN network. IFRP [98] adopts identity-preserving algorithms to help the GAN model produce high-quality face images with accurate identity information.

Since 2014, the attention mechanism has been gradually applied to visual tasks and has achieved great effects [106], [107]. The core idea of the attention mechanism is to reweight features through a learnable weight map to emphasize the important features and suppress the less useful ones. Many face restoration methods [91], [108], [109], [110] resort to the attention mechanism to improve their performance. Among them, [108], [109], [110] mainly design large-scale residual blocks with the attention mechanism to extract fine-grained face features, which can produce better performance. However, they do not consider cross-channel interaction in the residual blocks, which reduces the ability of feature representation in the network. Thus, Lu *et al.* [91] propose a split-attention in the split-attention network (SISN) for face super-resolution. SISN is stacked by several external-internal split attention group (ESAG) modules. ESAG uses multi-path learning, attention mechanism, and residual learning to enable the network to focus on facial texture details and structure information at the same time. With this specific module, SISN can generate high-quality faces containing more facial structural information. More Recently, the transformer has shown great potential in computer vision. Many methods [19], [65], [101], [102] aim to use strong transformer backbone to build



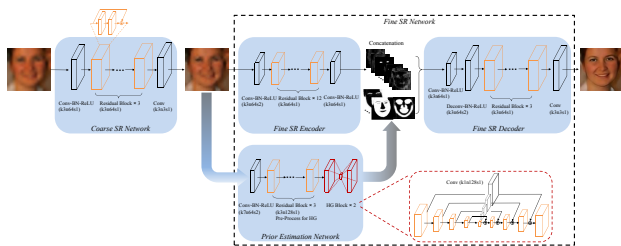


**Fig. 9:** Architecture to estimate face passing map in the middle of the network in [21].

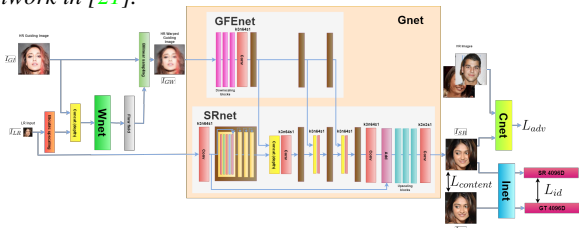


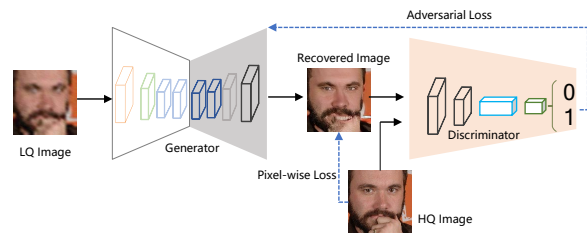
**Fig. 10:** Architecture to utilize the reference prior in the network in [73].

a prior estimation network respectively. After that, both image features and prior information are fed to the fine SR decoder to recover the final results.

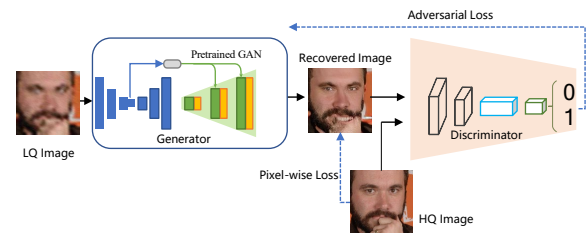
In contrast to the above methods that estimate face priors directly or indirectly from low-quality images, reference-prior face restoration methods aim to exploit the high-quality images of the same person to alleviate the difficulty of facial prior estimation or image restoration. Some methods [22], [73] propose a warping sub net to align the reference and degraded images. Typical works are GFRNet [22] and GWANet [73]. In GFRNet [22], a landmark loss and a total variation regularization is designed to train the warping sub net. As shown in Fig. 10, GWANet trains the warping sub net in an end-to-end manner without the facial landmark and proposes a feature fusion chain with multiple convolution layers to fuse features from the warped guidance and degraded image. Recent works [26], [29] propose to exploit deep facial component dictionaries or use multiple high-quality exemplars in the face restoration to exploit more guidance features and thus improve the generalization ability when dealing with low-quality face images with unknown degradation.

**GAN-based Networks.** With the success of the GAN architecture, some works aim at designing specialized GAN network for face restoration. As shown in Fig. 11, the architectures of GAN-based networks can be summarized as the plain GAN architecture and the pre-trained embedding architecture. In the plain GAN architecture-based methods [8], [18], [94], [95], [96], they introduce an adversarial loss in the network and use adversarial learning to jointly optimize the discriminator and generator (*i.e.*, face restoration network) to generate realistic face images. Among them, HLGAN [96] is one representative method for face super-resolution. As shown in Fig. 12, HLGAN consists of two generative adversarial networks. The first network is a High-to-Low GAN, which is trained with unpaired images to learn the degradation process of the high-resolution images. After that, its outputs (*i.e.*, low resolution face images) are adopted to train a Low-to-High GAN for face super-resolution. The second Low-to-High GAN is trained with paired face images. Thanks to this two-stage GAN architecture, HLGAN can achieve superior performance dealing with real face images.

In pre-trained GAN embedding architecture-based methods [9],



(a) Plain GAN architecture for face restoration



(b) Pre-trained GAN embedding architecture for face restoration

**Fig. 11:** Summary of GAN architecture used for face restoration. It mainly contains plain GAN architecture and pre-trained GAN embedding architecture.

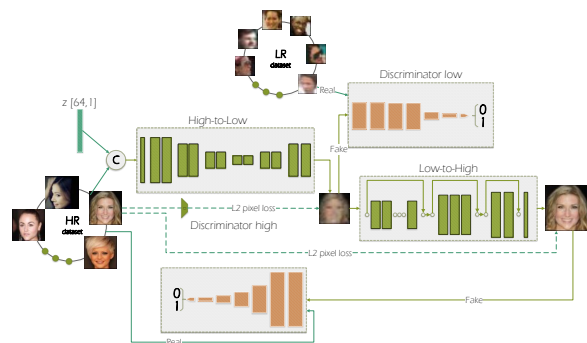


**Fig. 12:** The architecture of HLGAN [96], which is designed under the plain GAN architecture.

[23], [28], [99], [100], they exploit the latent prior in pre-trained face GAN models such as StyleGAN [80] and incorporate the prior into the process of face restoration. One representative work is GFP-GAN which effectively leverages face priors encapsulated in the pre-trained face GAN to perform the face restoration. The detail architecture of GFP-GAN [9] is illustrated in Fig. 13. Specifically, GFP-GAN is composed of a degradation removal module and a pre-trained face GAN. These modules are connected together by the latent code mapping and some Channel-Split Spatial Feature Transform layers. In addition, a loss function combined with the pixel-wise loss, the facial component loss, the adversarial loss, and the identity preserving loss is proposed to train the GFP-GAN. With these techniques, GFP-GAN can recover high-quality face images with facial details.

**ViT-based Network.** Recently, the Visual Transformer (ViT) [116] architecture has demonstrated superior performance in natural language processing and computer vision. ViT triggers the direct application of the Transformer architecture [117] in the computer vision tasks, including object recognition, detection, and classification [116], [118], [119]. ViT architecture also begins to be applied to the face restoration task. Wang *et al.* [19] propose RestorFormer based on ViT architecture for face restoration. RestorFormer aims at modeling contextual information of the face image to help the process of face restoration. Specifically, Wang *et*

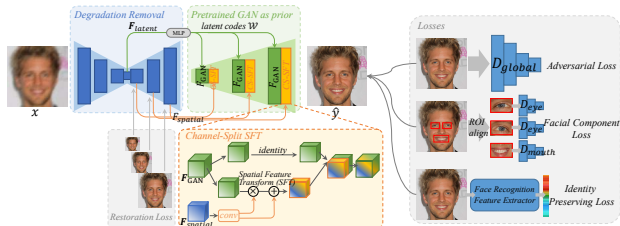


**Fig. 13:** The architecture of GFP-GAN [9], which is designed under the pre-trained GAN embedding architecture.

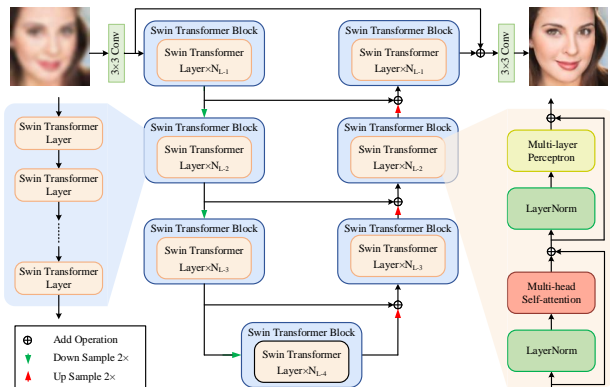


**Fig. 14:** The architecture of STUNet [65] that is built on swin transformer block.

*al.* propose a novel multi-head cross-attention layer, which explores spatial interactions between corrupted queries and high-quality key-value pairs. The high-quality key-value pairs are from a learned high-quality dictionary. With the help of advanced architecture and the high-quality dictionary prior, RestorFormer recovers results with more texture details and complete structures. Zhou *et al.* [102] treat face restoration as a code prediction task that aims at learning discrete codebook prior in a small finite proxy space. They thus propose a Transformer-based prediction network (CodeFormer) to achieve code prediction for face restoration.

To effectively process diverse scale face images, Li *et al.* [101] propose a novel scale-aware blind face restoration framework FaceFormer. They transform facial feature restoration as a facial scale-aware transformation procedure and then employ hierarchical transformer blocks in the network to extract robust facial features. The FaceFormer produces high-quality face images with faithful details. Inspired by the success of Swin transformer [120] on high-level vision tasks, Zhang *et al.* [65] propose an end-to-end Swin Transformer U-Net (STUNet) for face restoration, which is shown in Fig. 14. In STUNet, the self-attention mechanism and the shifted windowing scheme are used to help the model focus on important features for effective face restoration. Besides, they build two larger-scale face restoration benchmark datasets to further advance the development of face restoration and model evaluation. Although the above ViT based methods have demonstrated effectiveness in face restoration, there are still many problems to be studied, such as the model’s efficiency and generalization in real-world scenery.

## 4.2 Basic Blocks

In the field of face restoration, different types of basic blocks are designed to build powerful face restoration networks. In this section, we detail basic blocks that are widely used in the network.

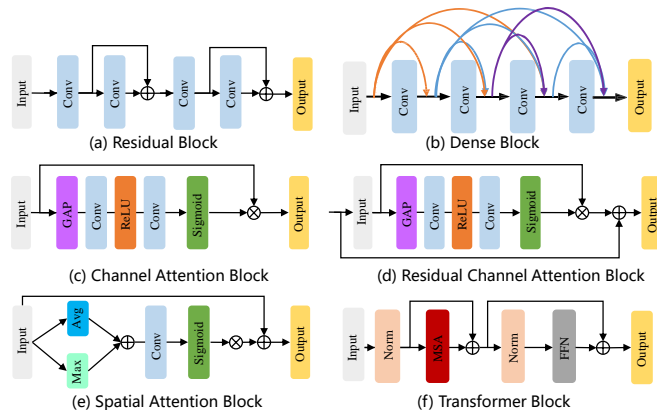


**Fig. 15:** Summary of basic blocks used in existing state-of-the-art networks.

### 4.2.1 Residual Learning

In 2016, He *et al.* [121] propose ResNet based on residual learning, and the residual block and corresponding residual learning have been widely used in vision tasks. The structure of residual block is shown in Fig. 15 (a). The residual block mainly consists of convolutional layers and residual connections. With the help of residual learning, the network can become deeper and it alleviates the problem of vanishing or exploding gradients in the training stage. Thus, many face restoration methods [21], [77], [78], [79] adopt the residual learning strategy to construct the network. We classify them into two types: global residual learning (GRL) and local residual learning (LRL).

**GRL Strategy.** This strategy is to model the residual image between the input image and the recovered image, which is effective in easing the difficulty of training the deep network [122]. Compared with directly predicting the clear image, it is easy for the network to learn the residual image where most regions are close to zero. Thus the GRL strategy is widely adopted in the network for face restoration [8], [65], [78].

**LRL Strategy.** This strategy is to use the residual connection in network modules or directly use the residual block to build the network. LRL can alleviate the problem of vanishing or exploding gradients in the training stage. Thus a larger number of face restoration methods use LRL when building the network [8], [9], [21], [27], [77], [79], [96]. For example, Chen *et al.* [21] use the residual block to build FSRNet for the face super-resolution task (Fig. 9). By choosing different numbers of residual blocks, they design a coarse SR network, a prior estimation network, a fine SR encoder, and a fine SR decoder, respectively. In FSRNet, these residual blocks work together to learn local and global features for better performance. In addition, some methods [8], [65], [90] combine GRL and LRL strategies in the model together to benefit from the advantages of both strategies.

### 4.2.2 Dense Connections

To alleviate gradient vanishing and encourage feature reuse in the network, Huang *et al.* [123] propose novel dense blocks to build a network called DenseNet, which has become a popular backbone in computer vision. As shown in Fig. 15 (b), each layer in the dense block processes features from all previous layers and its output features are sent to subsequent layers. The dense connections can help the network adaptively fuse multi-level features to generate detailed images and have been widely used in face restoration [68], [92], [124]. For example, Tu *et al.* [68] add dense connections in

the decoder of a network to reuse features from different spatial positions, which can help the network produce high-quality faces. Another representative work is DPDFN [92]. DPDFN combines residual connection, dense connection, and recursive techniques to build a basic residual dense recursive block to construct a global memory sub network. This sub network makes full use of the information from all the layers within it and helps DPDFN achieve better performance.

### 4.2.3 Attention Mechanism

With the successes of the attention mechanism in various vision tasks, the attention mechanism has been widely employed in face restoration networks [77], [79], [84]. Among them, the utilized attention techniques can be divided into channel attention, spatial attention, hybrid attention and other attention mechanism.

**Channel Attention.** The channel attention is to learn the relative weights between feature channels and make the model focus on the important feature channels. The basic channel blocks are shown in Fig. 15 (c-d). Chudasama *et al.* [90] propose an E-ComSupResNet network with channel attention to super-resolve low resolution face images. In E-ComSupResNet, it integrates the channel attention into the Resblock to rescale the channel-wise feature maps adaptively.

**Spatial Attention.** The spatial attention focuses on capturing spatial contextual information of the feature. The basic spatial attention is illustrated in Fig. 15 (e), which is explored in the face restoration [108], [124]. For instance, Chen *et al.* introduce a spatial attention mechanism to the residual blocks and use the modified block to build a network. With the guidance of spatial attention, the network can pay more attention to features related to the key face structures.

**Hybrid Attention.** Some methods use channel and spatial attention mechanisms to improve the representation of the network. For instance, to exploit the 3D face rendered priors in the network, Hu *et al.* [79] develop a Spatial Attention Module (SAM) with channel and spatial mechanisms to capture the locations of face components and the facial identity. This module effectively exploits the hierarchical information of 3D faces to help the network generate high-quality face images.

**Other Attention.** Some methods do not use the attention mechanism in the network design. On the contrary, they aim to propose attention-based loss to optimize the network. One representative work is PFSN [77], which uses facial heatmaps to produce a mask and obtains facial attention loss by computing the difference between the mask recovered and high-quality face images.

### 4.2.4 Transformer Block

Due to the strong capability in capturing long-range dependencies between sequences, recent transformer has been a popular architecture in the computer vision community. The vision transformer architecture usually decomposes an input image into a sequence of local windows and uses the self-attention mechanism to learn their relationships. We divide the transformer block into the plain transformer and swin transformer.

**Plain Transformer.** The original transformer block [116] is displayed in Fig. 15 (f). It contains a normalization layer, a multi-head self-attention layer, and a feed forward network layer. Recent methods [19], [102] employ the plain transformer block to build network modeling global interrelations. For example,

RestoreFormer [19] performs cross-self-attention mechanism between corrupted queries (extracted from input image) and high-quality key-value (sampled from high-quality dictionary) pairs by transformer blocks. With the help of transformer blocks, RestoreFormer can recover a clear face with realness and fidelity.

**Swin Transformer.** To reduce the complexity of the plain transformer, Liu *et al.* [120] propose the swin transformer layer to build an efficient Transformer network called Swin Transformer. The main difference between swin transformer layer and the plain transformer is that it adopts local attention and window shifting mechanism to realize multi-head self-attention. Due to its impressive performance, it has been used in the face restoration methods [65], [101]. Li *et al.* [101] use the swin transformer blocks in the network to effectively extract latent facial features. Zhang *et al.* [65] integrate the swin transformer block into the UNet network to learn hierarchical facial features, achieving state-of-the-art performance in the face restoration task.

## 4.3 Loss Functions

To optimize face restoration networks, numerous loss functions have been proposed in the literature. In general, loss functions used in the existing methods can be approximately divided into pixel-wise loss, perceptual loss, adversarial loss, and face-specific loss. We review these representative loss functions in the following.

**Pixel-wise Loss.** The pixel-wise loss measures the pixel-wise difference between the recovered image and its corresponding clear image. It can quickly match the feature distribution of restored and clear images and speed up network training. In existing methods, L1 and L2 losses are two widely-used pixel-wise losses in face restoration. They can be formulated as:

$$\mathcal{L}_1 = \frac{1}{CWH} \sum_{c=1}^C \sum_{x=1}^W \sum_{y=1}^H \|I_{hq(x,y,c)} - \hat{I}_{hq(x,y,c)}\|_1, \quad (8)$$

$$\mathcal{L}_2 = \frac{1}{CWH} \sum_{c=1}^C \sum_{x=1}^W \sum_{y=1}^H \|I_{hq(x,y,c)} - \hat{I}_{hq(x,y,c)}\|_2^2, \quad (9)$$

where  $I_{hq}$  and  $\hat{I}_{hq}$  represent the ground-truth and recovered face images respectively.  $W$  and  $H$  denote the size of the image.  $C$  refers to the channel of the image. It can be seen that L2 loss is only sensitive to large errors, while L1 loss treats larger and small errors equally. Early methods [21], [77], [85] usually use L2 loss in their models and recent works [19], [88], [100] mainly resort to L1 loss. While the pixel-wise loss can force the model to achieve high PSNR values, it often results in over-smooth and unrealistic images [33], [85].

**Perceptual Loss.** To generate more realistic high-quality face images, methods [4], [77], [85], [102] adopt a perceptual loss to train the network. The perceptual loss [25] computes the difference between the recovered image and the ground-truth image in the feature space of a pre-trained deep network such as VGG16, VGG19 [125], and ResNet [121]. The perceptual loss over a deep pre-trained network features at a given layer  $i$  is shown as:

$$\mathcal{L}_{\text{per}} = \frac{1}{C_i W_i H_i} \sum_{c=1}^{C_i} \sum_{x=1}^{W_i} \sum_{y=1}^{H_i} \left( \phi_i(I_{hq}) - \phi_i(\hat{I}_{hq}) \right)^2, \quad (10)$$

where  $\phi_i$  denotes the feature map obtained in the  $i$ -th layer of the pre-trained network, and  $W_i$ ,  $H_i$  represent the shape of the feature map.  $C_i$  is the channel number. Benefiting from the perceptual loss,

**TABLE 3:** Summary of loss functions used in existing face restoration methods.

Loss Function	Methods
L1 Loss	MFPSNet [88], GWAInet [73], GFP-GAN [9], GPEN [99], SGPNet [100], MSCNN [3], UMSN [4], RestoreFormer [19], FaceFormer [101], CodeFormer [102], VQFR [93], STUNet [65]
L2 Loss	FSRNet [21], Super-FAN [85], PFSN [77], FRN [79], PSFR-GAN [78], GFRNet [22], DFDNet [29], ASFFNet [26], mGANprior [23], MTUN [24], NPFNet [87], BCCNN [7], CBN [89], Attention-FH [84], TDAE [20], DeepDeblur [27], UR-DGN [18], MCGAN [94], TDN [95], HLGAN [96], HiFaceGAN [8]
Perceptual Loss	Super-FAN [85], PFSN [77], MFPSNet [88], mGANprior [23], MSCNN [3], UMSN [4], HiFaceGAN [8], CodeFormer [102], VQFR [93]
Adversarial Loss	FSRNet [21], Super-FAN [85], PFSN [77], PSFR-GAN [78], GFRNet [22], GWAInet [73], DFDNet [29], ASFFNet [26], GFP-GAN [9], GPEN [99], SGPNet [100], MSCNN [3], UMSN [4], NPFNet [87], UR-DGN [18], MCGAN [94], HiFaceGAN [8], CodeFormer [102], VQFR [93]
Face-specific Loss	Super-FAN [85], PFSN [77], FRN [79], PSFR-GAN [78], GFRNet [22], GFP-GAN [9], MSCNN [3], DeepDeblur [27]

face restoration methods [23], [85], [88] generate visually-pleasing results.

**Adversarial Loss.** The objective of GAN-based face restoration methods [9], [99], [100] is based on the min-max game. The core idea is to learn a generator  $\mathcal{G}$  to generate a high-quality face image such that discriminator  $\mathcal{D}$  cannot distinguish between the recovered image and the ground-truth image. This process can be expressed as solving the following min-max problem:

$$\min_{\mathcal{G}} \max_{\mathcal{D}} V(\mathcal{G}, \mathcal{D}) = E_{I_{hq} \sim p_{\text{train}}(I_{hq})} [\log(\mathcal{D}(I_{hq}))] + E_{I_{lq} \sim p_{\mathcal{G}}(I_{lq})} [\log(1 - \mathcal{D}(\mathcal{G}(I_{lq})))] , \quad (11)$$

where  $I_{hq}$  and  $I_{lq}$  are the high-quality face image and low-quality input image. The adversarial loss from the discriminator to optimize the generator is formulated as:

$$\mathcal{L}_{adv} = \log(1 - \mathcal{D}(\mathcal{G}(I_{lq}))) , \quad (12)$$

where  $\mathcal{D}(\mathcal{G}(I_{lq}))$  is the probability that the restored image is close to the ground truth image. With the help of adversarial loss, existing face restoration methods [8], [9], [99], [100] can generate realistic textures in the recovered face image.

**Face-specific Loss.** As a highly structured object, the human face has its own special characteristics, thus some face-related losses are used in face restoration. This kind of loss aims at incorporating information related to the structure of the human face into the face restoration process. The widely-used one is heatmap loss [77], [85], which is defined as:

$$\mathcal{L}_{\text{heatmap}} = \frac{1}{r^2 N W H} \sum_{n=1}^N \sum_{x=1}^{rW} \sum_{y=1}^{rH} (M_{x,y}^n - \tilde{M}_{x,y}^n)^2 , \quad (13)$$

where  $N$  represents the number of landmarks,  $M$  and  $\tilde{M}$  are face heatmaps that calculated from the ground-truth and restored images respectively. Some works introduce human identity loss in the model. The identity preserving loss [9] is shown as:

$$\mathcal{L}_{id} = \|\eta(\hat{I}_{hq}) - \eta(I_{hq})\|_1 , \quad (14)$$

where  $\eta$  is a face feature extractor, *e.g.*, ArcFace [137], which is used to capture features for identity discrimination. In addition, many other face-specific loss functions are proposed, including facial attention loss [77], face rendering loss [79], semantic-aware style loss [78], landmark loss [22], facial component loss [9], and

parsing loss [3]. A summary of loss functions used in previous works is listed in Table 3.

## 4.4 Datasets

In order to facilitate the training and evaluation of models, many benchmark datasets have been employed for face restoration. We provide the summary of the existing benchmark datasets in Table 4 and detail them in this part.

**BioID** [126] is created in 2001 and includes 1,521 gray-scale face images of 23 subjects.

**LFW** [127] is proposed by Huang *et al.* in 2008. Its full name is Labeled Faces in the Wild, including 13,233 images of 5,749 people. Compared with BioID, the distribution of images is more abundant in LFW.

**AFLW** [128] is a large-scale face alignment dataset collected from Flickr. It includes 25,993 face images annotated with up to 21 landmarks per image. The faces in this dataset contain various poses and expressions.

**Helen** [81] is a challenging facial feature localization dataset containing 2,330 high-resolution face images in the wild. This dataset provides 194 landmarks for each face image.

**300W** [129] is a facial landmark detection dataset that contains 3,837 images. In addition, 68 facial landmark points are provided for each face image.

**300W-LP** [130] is an expanded version of the 300W dataset. It generates more face images by rendering the faces from the original dataset with a larger variation of pose. It consists of 61,225 images from about 3,000 unique human faces.

**LS3D-W** [131] is a challenging 3D facial landmark dataset of approximately 230,000 face images.

**LS3D-W balanced** [131] is a subset of the LS3D-W [131] dataset and contains 7,200 images in total, where each pose range ( $[0^\circ - 30^\circ]$ ,  $[30^\circ - 60^\circ]$ ,  $[60^\circ - 90^\circ]$ ) is represented equally (2,400 images each). In this dataset, 4,200 face images are selected for training and 3,000 for testing.

**CASIA-WebFace** [132] is released in 2014. It consists of 494,414 face images from 10,575 different subjects. Each image is of  $250 \times 250$  resolution.

**CelebA** [67] is a face attribute dataset with face images sampled from the CelebFaces dataset [138]. It contains 202,599 face images with 10,177 unique human identities. And each image in CelebA is annotated with 40 face attributes and 5 key points. Based on the CelebA dataset, existing methods [9], [19], [26], [29] synthesize the CelebA-Test dataset for model evaluation. CelebA-Test is a synthetic dataset with 3,000 CelebA-HQ images from the testing set of CelebA.

**IMDB-WIKI** [133] consists of 524,230 face images collected from IMDB and Wikipedia websites in the Internet. Among them, 461,871 face images are obtained from IMDB, and 62,359 are crawled from the Wikipedia websites.

**VGGFace** [134] is released in 2015, which consists of 2.6 million images of 2,622 identities. This dataset is the largest-scale publicly available dataset when it is released.

**Menpo** [135] contains 8,979 face images. Moreover, this dataset also provides face images of different poses and provides corresponding 68-point landmarks or 39-point landmarks when some facial parts are not visible.

**VGGFace2** [136] is a large-scale face dataset, which includes 3.31 million images from 9,131 subjects. And each subject contains an average of 362.6 images in this dataset. The images

**TABLE 4:** Summary of benchmark datasets used in existing face restoration methods. – indicates that the resolution of the image is not fixed. HQ-LQ represents the pairs of low-quality and high-quality face images in the dataset.

Dataset	Size	Additional Label				Resolution	HQ-LQ
		Attributes	Landmarks	Parsing maps	Identity		
BioID [126]	1,521	✗	20	✗	✗	384 × 286	✗
LFW [127]	13,233	73	✗	✗	✓	250 × 250	✗
AFLW [128]	25,993	✗	21	✗	✗	–	✗
Helen [81]	2,330	✗	194	✓	✗	–	✗
300W [129]	3,837	✗	68	✗	✗	–	✗
300W-LP [130]	61,225	✗	✗	✗	✗	–	✗
LS3D-W [131]	230,000	✗	68	✗	✗	–	✗
LS3D-W balanced [131]	7,200	✗	68	✗	✗	–	✗
CASIA-WebFace [132]	494,414	✗	2	✗	✓	250 × 250	✗
CelebA [67]	202,599	40	5	✗	✓	–	✗
IMDB-WIKI [133]	524,230	✗	✗	✗	✗	–	✗
VGGFace [134]	2,600,000	✗	✗	✗	✓	–	✗
Menpo [135]	8,979	✗	68/39	✗	✗	–	✗
VGGFace2 [136]	3,310,000	✗	✗	✗	✓	–	✗
FFHQ [80]	70,000	✗	68	✗	✗	1024 × 1024	✗
EDFace-Celeb-1M [5]	1,700,000	✗	✗	✗	✗	–	✓
EDFace-Celeb-1M (BFR128) [65]	1,505,888	✗	✗	✗	✗	128 × 128	✓
EDFace-Celeb-150K (BFR512) [65]	148,962	✗	✗	✗	✗	512 × 512	✓

in VGGFace2 are collected from Google Image Search and have the characteristic of large variations in pose, age, and background. In addition, each face image in this dataset has a bounding box validated by a human around the face and five benchmark key points estimated by the model [139].

**FFHQ** [80] includes 70,000 high-quality human face images, which are crawled from Flickr. FFHQ is characterized by variability in age, ethnicity, and background, covering more human accessories such as glasses, sunglasses, and hats.

**EDFace-Celeb-1M** [5] is a new benchmark dataset for face super-resolution. Compared with existing face datasets, EDFace-Celeb-1M fully considers the distribution of human races in the process of building the dataset. It contains 1.7 million face images covering different human races from different countries. Specifically, this dataset provides pairs of low-resolution and high-resolution face images. There are 1.5 million pairs used for model training and testing and 140K real-world tiny face images for visual comparisons.

**EDFace-Celeb-1M (BFR128)** [65] is a benchmark dataset designed for blind face restoration. The high-quality images in this dataset are selected from EDFace-Celeb-1M [5]. Given high-quality images, the authors use degradation models (blur, noise, low resolution, JPEG compression artifacts, and full degradation) to synthesize low-quality images. With these different settings, this dataset can serve face deblurring, face denoising, face artifact removal, face super-resolution, and blind face restoration tasks. Specifically, each task contains 1.5 million images with resolution  $128 \times 128$ . And 1.36 million face images are used for training and 145,000 for testing.

**EDFace-Celeb-150K (BFR512)** [65] is another benchmark dataset for blind face restoration. The degradation of this dataset is the same as EDFace-Celeb-1M (BFR128) [65]. It also has five settings, including blur, noise, low resolution, JPEG compression artifacts, and a combination of them. EDFace-Celeb-150K (BFR512) contains 149K images of resolution  $512 \times 512$ . The number of training and testing images is about 132K and 17K respectively.

## 5 PERFORMANCE EVALUATION

In this section, we present a systematic benchmark evaluation of representative face restoration methods. Specifically, we first

describe the selected face restoration methods. Then, we introduce the experimental details. Finally, we discuss the benchmark results of the selected face restoration methods.

### 5.1 Representative Methods

To have a better understanding of existing deep learning-based face restoration methods, we choose different kinds of recent face restoration methods for performance evaluation on widely used benchmark datasets (including synthetic datasets EDFace-Celeb-1M (BFR128) [65], EDFace-Celeb-150k (BFR512) [65], CelebA-Test [67] and real-world datasets LFW-Test [127], CelebChild [9], WebPhoto [9]). We choose them as the code of the chosen methods is publicly available, and they cover all the categories discussed above. The chosen methods are shown as the following:

- 1) Deep Face Dictionary Network, DFDNet [29],
- 2) GAN Inversion Method, mGANprior [23],
- 3) Hierarchical Semantic Guidance GAN, HiFaceGAN [8],
- 4) Photo Upsampling via Latent Space Exploration, PULSE [28],
- 5) Progressive Semantic-aware Style Transformation Framework, PSFR-GAN [78],
- 6) GAN Prior Embedded Network, GPEN [99],
- 7) Generative Facial Prior GAN, GFP-GAN [9],
- 8) Swin Transformer U-Net, STUNet [65],
- 9) Transformer method with the multi-head cross-attention mechanism, RestoreFormer [19].

DFDNet [29] is a reference-based method that uses deep face component dictionaries to guide the process of face restoration. mGANprior [23] is a GAN inversion method, which employs multiple latent codes from the pre-trained GAN as generative prior to help the generator to restore a clear face image. HiFaceGAN [8] is a multi-stage framework that uses hierarchical semantic guidance for restoring face details. PULSE [28] is a method that achieves restoration via latent space learning. PSFR-GAN [78], GPEN [99] and GFP-GAN [9] are recent state-of-the-art GAN based methods. STUNet [65] and RestoreFormer [19] are new transformer based methods for face restoration.

### 5.2 Experimental Setting and Metric

**Setting.** To provide a clear view of existing face restoration methods, we use both synthetic datasets (EDFace-Celeb-1M

**TABLE 5: Performance comparison among representative BFR methods. The training sets are EDFace-Celeb-1M (BFR128) and EDFace-Celeb-150K (BFR512) respectively. The best and the second best performance values are highlighted and underlined respectively. Note that DFDN can only generate  $512 \times 512$  face results for any input image, thus we do not report its results on the EDFace-Celeb-1M (BFR128) dataset. The results are quoted from [65].**

Task	Methods	EDFace-Celeb-1M (BFR128)					EDFace-Celeb-150k (BFR512)				
		PSNR $\uparrow$	SSIM $\uparrow$	MS-SSIM $\uparrow$	LPIPS $\downarrow$	NIQE $\downarrow$	PSNR $\uparrow$	SSIM $\uparrow$	MS-SSIM $\uparrow$	LPIPS $\downarrow$	NIQE $\downarrow$
Face Deblurring	DFDNet [29]	—	—	—	—	—	25.4072	0.6512	0.8724	0.4008	<b>7.8913</b>
	HiFaceGAN [8]	22.4598	0.7974	0.9420	0.0739	<u>8.7261</u>	26.7421	<b>0.8095</b>	<b>0.9382</b>	<u>0.2029</u>	16.6642
	PSFR-GAN [78]	<b>29.1411</b>	<b>0.8563</b>	<b>0.9818</b>	0.0480	9.0008	27.4023	0.7604	0.9155	0.2292	17.4076
	GFP-GAN [9]	25.3822	0.7461	0.9534	<b>0.0704</b>	12.3608	28.8166	0.7709	0.9180	<b>0.1721</b>	15.5942
	GPEN [99]	24.9091	0.7307	0.9500	0.0887	<b>8.2288</b>	27.0658	0.7175	0.8928	0.2188	15.3187
	STUNet [65]	<u>27.3912</u>	<u>0.8080</u>	<u>0.9669</u>	0.2019	12.2652	<b>29.5572</b>	<u>0.8052</u>	<u>0.9289</u>	0.3381	<u>14.7874</u>
Face Denoising	DFDNet [29]	—	—	—	—	—	24.3618	0.5738	0.8423	0.3238	<b>7.7809</b>
	HiFaceGAN [8]	26.2976	0.8801	0.9663	0.0306	<b>7.2432</b>	30.0409	<u>0.8731</u>	0.9563	<u>0.1439</u>	16.7363
	PSFR-GAN [78]	<u>33.1007</u>	0.8563	0.9818	0.0480	9.0008	28.5397	0.8232	0.9390	0.2208	19.4719
	GFP-GAN [9]	31.1053	0.8802	0.9849	0.0234	<u>7.9522</u>	33.2020	0.8711	0.9582	<b>0.1259</b>	15.8440
	GPEN [99]	33.0744	<u>0.9086</u>	<u>0.9871</u>	<b>0.0211</b>	8.0616	32.3736	0.8517	0.9506	0.1555	<u>15.6820</u>
	STUNet [65]	<b>34.8914</b>	<b>0.9302</b>	<b>0.9900</b>	0.0331	8.5349	<b>34.5500</b>	<b>0.8848</b>	<b>0.9587</b>	0.1787	16.5480
Face Artifact Removal	DFDNet [29]	—	—	—	—	—	27.4781	0.7845	0.9409	0.2241	<b>7.5553</b>
	HiFaceGAN [8]	23.8228	0.8531	0.9567	0.0453	<b>7.6479</b>	27.1164	0.8897	0.9635	0.1241	18.7117
	PSFR-GAN [78]	<u>31.9455</u>	<u>0.8899</u>	<u>0.9887</u>	<b>0.0190</b>	8.3158	29.4285	0.9101	0.9719	0.1245	<u>15.9760</u>
	GFP-GAN [9]	31.0910	0.8804	0.9874	<u>0.0227</u>	<u>7.8027</u>	<u>35.7201</u>	<u>0.9144</u>	<u>0.9780</u>	<b>0.0842</b>	16.8320
	GPEN [99]	30.5753	0.8556	0.9837	0.0241	7.8074	33.8355	0.8701	0.9657	<u>0.0986</u>	16.9854
	STUNet [65]	<b>33.2082</b>	<b>0.9171</b>	<b>0.9912</b>	0.0582	10.5596	<b>36.5017</b>	<b>0.9246</b>	<b>0.9799</b>	0.1411	16.0487
Face Super-Resolution	DFDNet [29]	—	—	—	—	—	26.8691	0.7405	0.9224	0.2620	<b>7.4796</b>
	HiFaceGAN [8]	24.2965	<u>0.7792</u>	<u>0.9493</u>	0.0911	8.4801	26.6103	0.8480	0.9476	0.1681	15.8911
	PSFR-GAN [78]	23.9671	0.6858	0.9381	0.1364	<b>7.4807</b>	33.1233	0.8588	0.9602	<u>0.1331</u>	16.7143
	GFP-GAN [9]	<u>25.7118</u>	0.7558	0.9492	<b>0.0762</b>	11.4428	<u>33.4217</u>	<u>0.8629</u>	<u>0.9610</u>	<b>0.1127</b>	16.8970
	GPEN [99]	25.0208	0.7306	0.9448	<u>0.0843</u>	<u>7.9052</u>	31.3507	0.8273	0.9501	0.1357	<u>15.7813</u>
	STUNet [65]	<b>27.1206</b>	<b>0.8037</b>	<b>0.9566</b>	0.2018	12.7177	<b>33.9060</b>	<b>0.8809</b>	<b>0.9636</b>	0.2235	17.0899
Blind Face Restoration	DFDNet [29]	—	—	—	—	—	23.9349	0.5573	0.8053	0.4231	<b>9.0084</b>
	HiFaceGAN [8]	22.2179	<b>0.7088</b>	0.9128	0.1528	9.6864	25.3083	0.7260	<u>0.8701</u>	<u>0.3012</u>	14.7883
	PSFR-GAN [78]	22.2620	0.5199	0.8811	0.3558	<u>8.3706</u>	26.2998	0.6934	0.8581	0.3167	17.1906
	GFP-GAN [9]	<u>23.4159</u>	0.6707	0.9185	<b>0.1354</b>	12.6364	<b>28.4809</b>	<b>0.7857</b>	<b>0.9255</b>	<b>0.2171</b>	<u>14.4933</u>
	GPEN [99]	22.9731	0.6348	0.9119	<u>0.1387</u>	<b>8.0709</b>	25.5778	0.6721	0.8448	0.3113	15.8422
	STUNet [65]	<b>24.5500</b>	<u>0.6978</u>	<b>0.9225</b>	0.3523	13.0601	<u>27.1833</u>	<u>0.7346</u>	0.8654	0.4457	17.0305

(BFR128) [65], EDFace-Celeb-150k (BFR512) [65], FFHQ [80], and CelebA-Test [67]) and real-world datasets (LFW-Test, CelebChild-Test, and WebPhoto-Test [9]) for training and evaluation. Specifically, we conduct two different experimental settings for model training and testing. We detail them as follows.

**Experimental Scheme One:** EDFace-Celeb-1M (BFR128) and EDFace-Celeb-150k (BFR512) provide five degradation settings corresponding to face deblurring, face denoising, face artifact removal, face super-resolution, and blind face restoration tasks. We adopt the code and pre-trained models provided in [65]. For a fair comparison, these methods are first trained with the same configurations (*e.g.*, same number of epochs) on the training sets of EDFace-Celeb-1M (BFR128) and EDFace-Celeb-150k (BFR512) respectively. Then, the trained models are evaluated on the testing sets of EDFace-Celeb-1M (BFR128) and EDFace-Celeb-150k (BFR512) respectively.

**Experimental Scheme Two:** In [9], [19], [29], they first synthesize degraded face images on the FFHQ [80] dataset via the degradation model described in Eq. 7. In the degradation model, the parameters  $\sigma$ ,  $\delta$ ,  $r$  and  $q$  are randomly sampled from  $\{0.2 : 10\}$ ,  $\{1 : 8\}$ ,  $\{0 : 20\}$ , and  $\{60 : 100\}$ , respectively. Then, they use paired face images to train networks. In addition, one synthetic dataset (CelebA-Test [67]) and three real-world datasets (LFW-Test, CelebChild-Test, and WebPhoto-Test [9]) are used as testing datasets to measure the performance of models. Note that these testing sets have no overlap with the FFHQ dataset.

**Metric.** The full-reference and non-reference metrics are employed to benchmark these methods in the experiments. The full-reference metrics contain PSNR, SSIM, MS-SSIM, and LPIPS. These full-reference metrics measure the visual quality in different aspects, including pixels, structure, and human perception. The non-reference metrics consist of NIQE and FID, which can be used for real-world datasets without ground truth.

### 5.3 Quantitative Evaluation

We evaluate several state-of-the-art face restoration methods on both the synthetic and real-world datasets quantitatively regarding tasks including face deblurring, face denoising, face artifact removal, face super-resolution, and blind face restoration.

Table 5 reports the quantitative results of six face restoration methods on the EDFace-Celeb-1M and EDFace-Celeb-150K datasets, where face deblurring, face denoising, face artifact removal, face super-resolution, and blind face restoration refer to five face restoration tasks related to the degradation from blur, noise, JPEG, low resolution, and a mix of them, respectively. For the comparison results in terms of PSNR, SSIM, MS-SSIM, LPIPS, NIQE, we have the following findings. (i) In terms of PSNR, SSIM, and MS-SSIM, the transformer-based method STUNet is very competitive and outperforms the best face prior based methods. Specifically, STUNet achieves the best performance on face denoising, face artifact removal, and face super-resolution tasks, and it also achieves the second best performance in face deblurring and blind face restoration tasks. Compared with other face restoration methods (DFDNet, HiFaceGAN, PSFR-GAN, GFP-GAN, GPEN), though STUNet does not explicitly consider the face related prior, it still achieves outstanding performance in many face restoration tasks. It demonstrates that it is very important to choose a reasonable network architecture, and a well-designed architecture will easily result in stronger performance. This observation will inspire us to design deep networks based on a strong backbone network. (ii) In terms of LPIPS and NIQE (non-reference quantitative metrics), GFP-GAN and GPEN achieve the best or second best performance for most face tasks, and HiFaceGAN and PSFR-GAN place the best or second best on some face tasks. Compared with STUNet, GAN-based methods (HiFaceGAN, PSFR-GAN, GFP-GAN, and GPEN) obtain better

**TABLE 6:** Quantitative comparisons on CelebA-Test in terms of FID, PSNR, SSIM, and LPIPS. The red and blue colors indicate the best and the second best performance. For a fair comparison, all models are finetuned or trained on face images synthesized from FFHQ [80].

Methods	FID↓	PSNR↑	SSIM↑	LPIPS↓
Input	132.69	24.96	0.6624	0.4989
DFDNet [29]	52.92	24.10	0.6092	0.4478
PSFR-GAN [78]	43.88	<b>24.45</b>	0.6308	0.4186
PULSE [28]	67.75	21.61	0.6287	0.4657
GFP-GAN [9]	<b>42.39</b>	<b>24.46</b>	<b>0.6684</b>	<b>0.3551</b>
RestoreFormer [19]	<b>41.45</b>	24.42	<b>0.6404</b>	<b>0.3650</b>

**TABLE 7:** Quantitative comparison on the real-world datasets of LFW-Test, CelebChild-Test, and WebPhoto-Test. The red and blue colors indicate the best and the second best performance. For a fair comparison, all models are finetuned or trained on images synthesized from FFHQ [80].

Dataset Methods	LFW-Test		CelebChild		WebPhoto	
	FID↓	NIQE↓	FID↓	NIQE↓	FID↓	NIQE↓
Input	137.56	11.214	144.42	9.170	170.11	12.755
HiFaceGAN [8]	64.50	4.510	113.00	4.855	116.12	4.885
DFDNet [29]	62.57	<b>4.026</b>	111.55	<b>4.414</b>	100.68	5.293
PSFR-GAN [78]	51.89	5.096	107.40	4.804	88.45	5.582
mGANprior [23]	73.00	6.051	126.54	6.841	120.75	7.226
PULSE [28]	64.86	5.097	<b>102.74</b>	5.225	<b>86.45</b>	5.146
GFP-GAN [9]	<b>49.96</b>	<b>3.882</b>	111.78	<b>4.349</b>	87.35	<b>4.144</b>
RestoreFormer [19]	<b>47.75</b>	4.168	<b>101.22</b>	4.582	<b>77.33</b>	<b>4.459</b>

performance. Because GAN based methods are good at generating content pleasing the human visual perception system, easily achieving better performance on non-reference quantitative metrics. This suggests that we should consider more different metrics when carrying out the performance evaluation.

The quantitative results of CelebA-Test [67] dataset are shown in Table 6. On this testing dataset, GFP-GAN and RestoreFormer achieve competitive performance. Specifically, GFP-GAN and RestoreFormer obtain lower FID and NIQE, which demonstrates the restored face has a close distance with the real face distribution. In addition, GFP-GAN and RestoreFormer obtain higher PSNR and SSIM, showing that the recovered face images are more similar to the ground-truth face images in the image pixel aspect. To further evaluate the generalization of existing face restoration methods, we also apply the existing methods on real-world datasets, including LFW-Test, CelebChild-Test, and WebPhoto-Test [9]. Table 7 reports the quantitative results in terms of FID and NIQE. The recent transformer-based method RestoreFormer obtains the best performance in these dataset in terms of FID. GFP-GAN achieves the best performance in these dataset in terms of NIQE. The experiments show that the results of FID and NIQE are not always consistent. Therefore, the study of face restoration performance evaluation is of great significance for future work.

## 5.4 Qualitative Evaluation

To evaluate the visual quality of existing state-of-the-art methods, we also conduct qualitative experiments on both synthetic and real-world datasets. The comparison methods include DFDNet [29], HiFaceGAN [8], PSFR-GAN [78], GPEN [99], PULSE [28], STUNet [65], GFP-GAN [9], and RestoreFormer [19].

Fig. 16 and 17 show the visual results of face deblurring, face denoising, face artifact removal, face super-resolution, and blind face restoration on EDFace-Celeb-1M and EDFace-Celeb-150K datasets, respectively. We can see that face images generated by the GAN-based methods (DFDNet, HiFaceGAN, PSFR-GAN, and GPEN) are more visual-pleasing by human visual perception. For example, for face deblurring in the EDFace-Celeb-1M dataset,

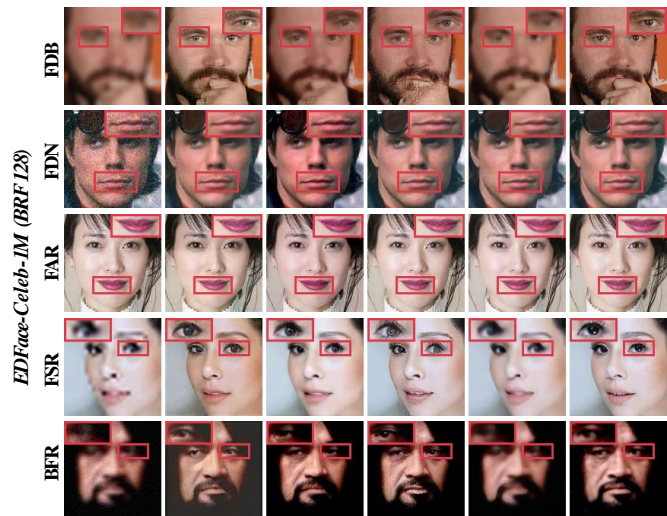


**Fig. 16:** Visual comparison on the EDFace-Celeb-1M (BFR 128) dataset. FDB, FDN, FAR, FSR and BFR indicate face deblurring, face denoising, face artifact removal, face super-resolution, and face restoration, respectively. From left to right are the input, the results of HiFaceGAN, PSFR-GAN, GPEN and STUNet, and HQ images. **Zoom in for details.**

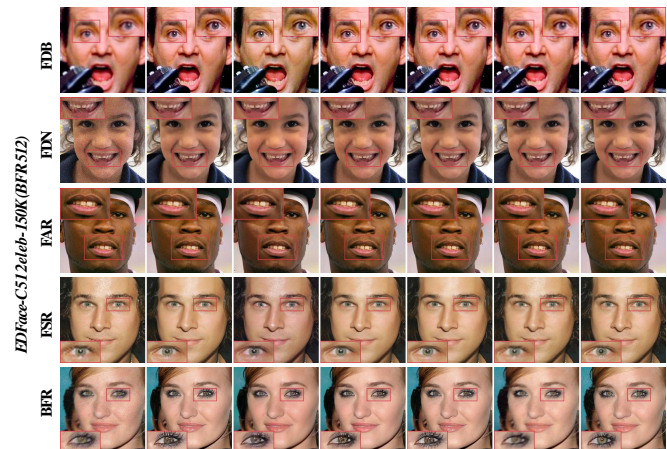


**Fig. 17:** Visual comparison on the EDFace-Celeb-150K (BFR512) dataset. FDB, FDN, FAR, FSR, BFR indicate face deblurring, face denoising, face artifact removal, face super-resolution, and blind face restoration, respectively. From left to right are the input, the results of DFDNet, HiFaceGAN, PSFR-GAN, GPEN and STUNet, and HQ images. **Zoom in for details.**

HiFaceGAN and GPEN can effectively remove the blur in face images, STUNet cannot deal with the blur well (see the eyes in the first row of Fig. 16). For the most challenging task of blind face restoration, we find that GPEN generates visually more pleasing face images (see the woman’s eyes in the last row of Fig. 17). The visual results are more consistent with the results of the non-reference metrics. Therefore, non-reference indicators (e.g., NIQE, FID) should be fully considered in the performance evaluation.

Fig. 18 presents the visual results on the set of CelebA-Test. In the figure, PULSE can recover face images well. However, it changes the human identity compared with GFP-GAN and RestoreFormer. DFDNet and PSFR-GAN cannot recover details of faces well (see the left eyebrow in the first row and the eyeglasses marked blue box in the second row). The recent state-of-the-art method RestoreFormer could generate plausible face images. We also apply the methods on the real-world datasets to evaluate their

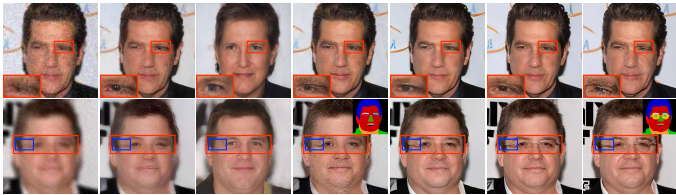


**Fig. 18:** Visual comparison on *CelebA-Test*, which is quoted from [19]. From left to right are the input, the results of DFDNet, PULSE, PSFR-GAN, GFP-GAN and RestoreFormer, and HQ images. Zoom in for a better view.



**Fig. 19:** Visual comparison on real-world *LFW-Test*, *CelebChild-Test*, *WebPhoto-Test* datasets. From left to right are the input, the results of HiFaceGAN, DFDNet, PSFR-GAN, PULSE, GFP-GAN, and RestoreFormer. Zoom in for details.

generalization ability. The qualitative comparisons are shown in Fig. 19. GFP-GAN and RestoreFormer can generate realistic faces in real complex scenes, while other methods fail to restore the details and color of the face components (see the woman’s teeth in the second row and the girl’s eyes in the last row). Though RestoreFormer can recover the details well, it cannot conduct color enhancement well in some recovered face images (see the fifth and sixth rows). In general, GFP-GAN with generative face priors has better generalization ability in real scenarios.

## 5.5 Computational Complexity

Table 8 shows the running time and overhead of the existing state-of-the-art methods. All methods are implemented in the same computer using one GPU. From the comparison results, we find that the inference speed of GPEN and PSFR-GAN is faster than that of other methods, and STUNet has the fewest parameters. In addition to GPEN, other methods have high computational complexity (see MACs). In general, the existing state-of-the-art face restoration methods are complex. In the future, we expect more work on designing light-weighted face restoration models for edge devices.

## 6 FUTURE DIRECTIONS

Despite great breakthroughs in face restoration technology, there still exist many challenges and unsolved problems. In this section,

**TABLE 8:** Running time and overhead comparison of typical face restoration methods. The numbers of parameters (Param) and multiply-accumulate operations (MACs) are used to compute the overhead. MACs are measured on  $512 \times 512$  images. We test models with a PC using an NVIDIA GeForce 3060 GPU for fair comparisons.

Method	DFDNet [29]	HiFaceGAN [8]	PSFR-GAN [78]
Speed (sec.)	0.66	0.16	0.04
Params (M)	133.34	130.54	45.69
MACs(G)	608.74	697.70	102.80
GFP-GAN [9]	GPEN [99]	STUNet [65]	RestoreFormer [19]
0.06	0.04	0.17	0.06
60.76	26.23	24.81	72.37
85.04	17.78	334.25	340.80

we discuss the limitations of existing methods and introduce new trends for future works.

## 6.1 Network Design

As discussed in the performance evaluation, the network structure can significantly influence the restoration performance. For example, recent transformer-based methods usually have better performance due to the strong ability of transformer architecture. GAN-based methods can generate visual-pleasing face images with better non-reference metric values. Thus, when designing the network, it is worthwhile to learn from different structures, including CNN, GAN, and ViT. On the other hand, recent transformer-based models often require high computation costs and larger parameters, which makes them difficult to be deployed in edge devices. Thus, how to design a lightweight network with strong performance is another potential research direction in future work.

## 6.2 Integration of Facial Priors and Networks

As a domain-specific image restoration task, the facial features can be used in the face restoration task. When designing models, many methods aim at exploiting facial priors to recover realistic face details. Although some methods attempt to introduce geometry prior, facial component, generative prior, or 3D prior into face restoration, how to integrate the prior information into networks is still a promising direction for this task. In addition, exploiting new face-related priors such as priors from pre-trained GAN or data statistics in networks, is another direction for this task.

## 6.3 Loss Function and Evaluation Metrics

For the face restoration task, different loss functions have been adopted in the literature. The widely-used loss functions are L1 loss, L2 loss, perceptual loss, adversarial loss, and face-specific loss, which are shown in Table 3. Instead of using a single loss function, existing methods usually combine multiple loss functions with corresponding weights to train models. However, it is still not clear how to develop the right loss function for guiding the model training. Thus in the future, more works are expected to seek more accurate loss functions (*e.g.*, general or task-driven loss functions) to promote the development of face restoration. In addition, loss functions can directly influence the evaluation results of models. As shown in Table 5, 6, and 7, the pixel-wise L1 loss and L2 Loss tend to obtain better results in terms of PSNR, SSIM and, MS-SSIM. The perceptual loss and adversarial loss tend to generate more visual-pleasing results (*i.e.*, producing high LPIPS, FID, and NIQE values). Thus, how to develop metrics that can consider both human and machine aspects for model evaluation is also an important direction in the future.

## 6.4 Computational Cost

Existing face restoration methods aim at improving the restoration performance via significantly increasing the depth or width of the network, ignoring the computational cost of models. The heavy computational cost prevents these methods from being used in resource-limited environments, such as mobile or embedded devices. For example, as shown in Table 8, the state-of-the-art method RestoreFormer [19] has 72.37M parameters and 340.80G MACs. It is very difficult to deploy it in real-world applications. Therefore, developing models with a lighter computational cost is an important future direction.

## 6.5 Standard Benchmark Datasets

Unlike other low-level visual tasks such as image deblurring, image denoising, and image dehazing, there are few standard evaluation benchmarks for face restoration [65]. For example, most face restoration methods [9], [19], [29] conduct experiments on private datasets (synthesizing the training set from FFHQ). Researchers may tend to use data that is biased to their proposed methods. On the other hand, to make a fair comparison, subsequent works need to take a lot of time to synthesize private data sets and retrain other comparison methods. In addition, the scale of the recent widely-use dataset is usually small, which is not suitable for deep learning methods. Thus, developing standard benchmark datasets is a direction for the face restoration task. In the future, we expect more standard and high-quality benchmark datasets to be built by researchers in the community.

## 6.6 Video Face Restoration

With the popularization of mobile phones and cameras, the video face restoration task has become more and more important. However, existing works mainly focus on image-level face restoration, and there are few video-related works for face restoration. On the other hand, other low-level visual tasks such as video deblurring, video super-resolution, and video denoising have developed rapidly in recent years. Therefore, video face restoration is a potential direction for the community. The task of video face restoration can be considered from the following two aspects. First, for the benchmark dataset, we could consider building high-quality video datasets for this task, which can quickly facilitate algorithm design and evaluation and benefit the community of face restoration. Second, for video restoration methods, we should develop video-based face restoration by fully considering the spatial and temporal information among successive frames.

## 6.7 Real-world Face Restoration and Application

Existing methods rely on synthetic data to train networks. However, the trained networks cannot necessarily perform well in real-world scenarios. As shown in Fig. 19, most of face restoration methods produce poor results when dealing with real-world face images. Because there is a natural domain gap between synthetic data and real world data. Some solutions are introduced to solve this problem, such as unsupervised techniques or learning real image degradation techniques. However, they still rely on some specific assumptions that all images have similar degradation. Thus, the real-world application is still a challenging direction for the task of face restoration. In addition, some methods [3], [92] have shown that face restoration can improve the performance of subsequent tasks such as face verification and face recognition. However, how to couple face restoration with these tasks in a framework is a future research direction.

## 6.8 Other Related Tasks

Except the above-discussed face restoration tasks, there are many tasks related to face restoration, including face retouching [140], photo-sketch synthesis [141], face-to-face translation [142], face inpainting [100], color enhancement [102] and old photo restoration [143]. For example, face inpainting aims to recover the missing regions of a face image by matching or learning. It not only requires generating new pixels for missing facial components semantically, but also should maintain consistency in facial structure and appearance. Old photo restoration is the task to repair old photos, where the degradation of old photos is rather diverse and complex (e.g., noise, blur, and color fading). In addition, some tasks focus on facial style transfer, such as face-to-face translation and facial expression analysis, which are different from face restoration. Thus, applying the existing face restoration methods into these related tasks is also a promising direction, which can trigger more application tasks landing.

## 7 CONCLUSION

In this work, we have systematically surveyed face restoration methods using deep learning. We discuss different degradation models, the characteristics of face images, the challenges of face restoration, and the core ideas in existing state-of-the-art methods, including geometric prior based methods, reference prior based methods, generative prior based methods, and non-prior based methods. After comprehensively reviewing face restoration methods, we discuss advanced techniques in face recovery methods from aspects of network architecture, basic block, loss function, and benchmark dataset. We also evaluate the representative methods on synthetic and real-world datasets. Finally, we discuss the future directions, including network design, metrics, benchmark datasets, applications, etc.

## REFERENCES

- [1] E. Luo, S. H. Chan, and T. Q. Nguyen, "Adaptive image denoising by targeted databases," *IEEE Transactions on Image Processing*, vol. 24, no. 7, pp. 2167–2181, 2015.
- [2] S. Anwar, F. Porikli, and C. P. Huynh, "Category-specific object image denoising," *IEEE Transactions on Image Processing*, vol. 26, no. 11, pp. 5506–5518, 2017.
- [3] Z. Shen, W.-S. Lai, T. Xu, J. Kautz, and M.-H. Yang, "Exploiting semantics for face image deblurring," *International Journal of Computer Vision*, vol. 128, no. 7, pp. 1829–1846, 2020.
- [4] R. Yasarla, F. Perazzi, and V. M. Patel, "Deblurring face images using uncertainty guided multi-stream semantic networks," *IEEE Transactions on Image Processing*, vol. 29, pp. 6251–6263, 2020.
- [5] K. Zhang, D. Li, W. Luo, J. Liu, J. Deng, W. Liu, and S. Zafeiriou, "Edface-celeb-1 m: Benchmarking face hallucination with a million-scale dataset," *IEEE Transactions on Pattern Analysis and Machine Intelligence*, 2022.
- [6] S. Baker and T. Kanade, "Hallucinating faces," in *Proceedings of the IEEE International Conference on Automatic Face and Gesture Recognition*, 2000, pp. 83–88.
- [7] E. Zhou, H. Fan, Z. Cao, Y. Jiang, and Q. Yin, "Learning face hallucination in the wild," in *Proceedings of the AAAI Conference on Artificial Intelligence*, 2015.
- [8] L. Yang, S. Wang, S. Ma, W. Gao, C. Liu, P. Wang, and P. Ren, "Hifacegan: Face renovation via collaborative suppression and replenishment," in *Proceedings of the ACM International Conference on Multimedia*, 2020, pp. 1551–1560.
- [9] X. Wang, Y. Li, H. Zhang, and Y. Shan, "Towards real-world blind face restoration with generative facial prior," in *Proceedings of the IEEE Conference on Computer Vision and Pattern Recognition*, 2021, pp. 9168–9178.
- [10] S. Z. Li and Z. Zhang, "Floatboost learning and statistical face detection," *IEEE Transactions on Pattern Analysis and Machine Intelligence*, vol. 26, no. 9, pp. 1112–1123, 2004.

- [11] J. Yu, B. Zhang, Z. Kuang, D. Lin, and J. Fan, "Iprivacy: image privacy protection by identifying sensitive objects via deep multi-task learning," *IEEE Transactions on Information Forensics and Security*, vol. 12, no. 5, pp. 1005–1016, 2016.
- [12] C. Chen, A. Seff, A. Kornhauser, and J. Xiao, "Deepdriving: Learning affordance for direct perception in autonomous driving," in *Proceedings of the IEEE International Conference on Computer Vision*, 2015, pp. 2722–2730.
- [13] X. Tang and X. Wang, "Face sketch synthesis and recognition," in *Proceedings of the IEEE International Conference on Computer Vision*, 2003, pp. 687–694.
- [14] Y.-h. Li, M. Savvides, and V. Bhagavatula, "Illumination tolerant face recognition using a novel face from sketch synthesis approach and advanced correlation filters," in *Proceedings of the IEEE International Conference on Acoustics Speech and Signal Processing Proceedings*, 2006.
- [15] X. He and P. Niyogi, "Locality preserving projections," in *Proceedings of Advances in Neural Information Processing Systems*, 2003.
- [16] N. Wang, X. Gao, D. Tao, and X. Li, "Face sketch-photo synthesis under multi-dictionary sparse representation framework," in *Proceedings of International Conference on Image and Graphics*, 2011, pp. 82–87.
- [17] L. Tian, C. Fan, Y. Ming, and X. Hong, "Weighted non-locally self-similarity sparse representation for face deblurring," in *Proceedings of Asian Conference on Computer Vision*, 2016, pp. 576–589.
- [18] X. Yu and F. Porikli, "Ultra-resolving face images by discriminative generative networks," in *Proceedings of the European Conference on Computer Vision*, 2016, pp. 318–333.
- [19] Z. Wang, J. Zhang, R. Chen, W. Wang, and P. Luo, "Restoreformer: High-quality blind face restoration from degraded key-value pairs," in *Proceedings of the IEEE Conference on Computer Vision and Pattern Recognition*, 2022, pp. 17 512–17 521.
- [20] X. Yu and F. Porikli, "Hallucinating very low-resolution unaligned and noisy face images by transformative discriminative autoencoders," in *Proceedings of the IEEE Conference on Computer Vision and Pattern Recognition*, 2017, pp. 3760–3768.
- [21] Y. Chen, Y. Tai, X. Liu, C. Shen, and J. Yang, "Fsrnet: End-to-end learning face super-resolution with facial priors," in *Proceedings of the IEEE Conference on Computer Vision and Pattern Recognition*, 2018, pp. 2492–2501.
- [22] X. Li, M. Liu, Y. Ye, W. Zuo, L. Lin, and R. Yang, "Learning warped guidance for blind face restoration," in *Proceedings of the European Conference on Computer Vision*, 2018, pp. 272–289.
- [23] J. Gu, Y. Shen, and B. Zhou, "Image processing using multi-code gan prior," in *Proceedings of the IEEE Conference on Computer Vision and Pattern Recognition*, 2020, pp. 3012–3021.
- [24] X. Yu, B. Fernando, B. Ghanem, F. Porikli, and R. Hartley, "Face super-resolution guided by facial component heatmaps," in *Proceedings of the European Conference on Computer Vision*, 2018, pp. 217–233.
- [25] J. Johnson, A. Alahi, and L. Fei-Fei, "Perceptual losses for real-time style transfer and super-resolution," in *Proceedings of the European Conference on Computer Vision*, 2016, pp. 694–711.
- [26] X. Li, W. Li, D. Ren, H. Zhang, M. Wang, and W. Zuo, "Enhanced blind face restoration with multi-exemplar images and adaptive spatial feature fusion," in *Proceedings of the IEEE Conference on Computer Vision and Pattern Recognition*, 2020, pp. 2706–2715.
- [27] L. Wang, Y. Li, and S. Wang, "Deepdeblur: fast one-step blurry face images restoration," *arXiv preprint arXiv:1711.09515*, 2017.
- [28] S. Menon, A. Damian, S. Hu, N. Ravi, and C. Rudin, "Pulse: Self-supervised photo upsampling via latent space exploration of generative models," in *Proceedings of the IEEE Conference on Computer Vision and Pattern Recognition*, 2020, pp. 2437–2445.
- [29] X. Li, C. Chen, S. Zhou, X. Lin, W. Zuo, and L. Zhang, "Blind face restoration via deep multi-scale component dictionaries," in *Proceedings of the European Conference on Computer Vision*, 2020, pp. 399–415.
- [30] W. Yang, R. T. Tan, S. Wang, Y. Fang, and J. Liu, "Single image deraining: From model-based to data-driven and beyond," *IEEE Transactions on Pattern Analysis and Machine Intelligence*, vol. 43, no. 11, pp. 4059–4077, 2020.
- [31] C. Tian, L. Fei, W. Zheng, Y. Xu, W. Zuo, and C.-W. Lin, "Deep learning on image denoising: An overview," *Neural Networks*, vol. 131, pp. 251–275, 2020.
- [32] Z. Wang, J. Chen, and S. C. Hoi, "Deep learning for image super-resolution: A survey," *IEEE Transactions on Pattern Analysis and Machine Intelligence*, vol. 43, no. 10, pp. 3365–3387, 2020.
- [33] K. Zhang, W. Ren, W. Luo, W.-S. Lai, B. Stenger, M.-H. Yang, and H. Li, "Deep image deblurring: A survey," *International Journal of Computer Vision*, vol. 130, no. 9, pp. 2103–2130, 2022.
- [34] J. Su, B. Xu, and H. Yin, "A survey of deep learning approaches to image restoration," *Neurocomputing*, vol. 487, pp. 46–65, 2022.
- [35] Y. Liang, J.-H. Lai, W.-S. Zheng, and Z. Cai, "A survey of face hallucination," in *Proceedings of Chinese Conference on Biometric Recognition*, 2012, pp. 83–93.
- [36] N. Wang, D. Tao, X. Gao, X. Li, and J. Li, "A comprehensive survey to face hallucination," *International Journal of Computer Vision*, vol. 106, no. 1, pp. 9–30, 2014.
- [37] K. Nguyen, C. Fookes, S. Sridharan, M. Tistarelli, and M. Nixon, "Super-resolution for biometrics: A comprehensive survey," *Pattern Recognition*, vol. 78, pp. 23–42, 2018.
- [38] S. S. Rajput, K. Arya, V. Singh, and V. K. Bohat, "Face hallucination techniques: A survey," in *Proceedings of Conference on Information and Communication Technology*, 2018, pp. 1–6.
- [39] H. Liu, X. Zheng, J. Han, Y. Chu, and T. Tao, "Survey on gan-based face hallucination with its model development," *IET Image Processing*, vol. 13, no. 14, pp. 2662–2672, 2019.
- [40] J. Jiang, C. Wang, X. Liu, and J. Ma, "Deep learning-based face super-resolution: A survey," in *Proceedings of the ACM Computing Surveys*, 2021, pp. 1–36.
- [41] S. Anwar and N. Barnes, "Real image denoising with feature attention," in *Proceedings of the IEEE International Conference on Computer Vision*, 2019, pp. 3155–3164.
- [42] Z. Yue, H. Yong, Q. Zhao, D. Meng, and L. Zhang, "Variational denoising network: Toward blind noise modeling and removal," in *Proceedings of Advances in Neural Information Processing Systems*, 2019.
- [43] O. Kupyn, V. Budzan, M. Mykhailych, D. Mishkin, and J. Matas, "Deblurgan: Blind motion deblurring using conditional adversarial networks," in *Proceedings of the IEEE Conference on Computer Vision and Pattern Recognition*, 2018, pp. 8183–8192.
- [44] W. Yang, X. Zhang, Y. Tian, W. Wang, J.-H. Xue, and Q. Liao, "Deep learning for single image super-resolution: A brief review," *IEEE Transactions on Multimedia*, vol. 21, no. 12, pp. 3106–3121, 2019.
- [45] C. Dong, C. C. Loy, K. He, and X. Tang, "Image super-resolution using deep convolutional networks," *IEEE Transactions on Pattern Analysis and Machine Intelligence*, vol. 38, no. 2, pp. 295–307, 2015.
- [46] B. Lim, S. Son, H. Kim, S. Nah, and K. Mu Lee, "Enhanced deep residual networks for single image super-resolution," in *Proceedings of the IEEE Conference on Computer vision and Pattern Recognition Workshops*, 2017, pp. 136–144.
- [47] X. Wang, K. Yu, S. Wu, J. Gu, Y. Liu, C. Dong, Y. Qiao, and C. Change Loy, "Esrgan: Enhanced super-resolution generative adversarial networks," in *Proceedings of the European Conference on Computer Vision Workshops*, 2018, pp. 0–0.
- [48] C. Dong, Y. Deng, C. C. Loy, and X. Tang, "Compression artifacts reduction by a deep convolutional network," in *Proceedings of the IEEE International Conference on Computer Vision*, 2015, pp. 576–584.
- [49] J. Liu, D. Liu, W. Yang, S. Xia, X. Zhang, and Y. Dai, "A comprehensive benchmark for single image compression artifact reduction," *IEEE Transactions on Image Processing*, vol. 29, pp. 7845–7860, 2020.
- [50] K. Zhang, W. Luo, Y. Zhong, L. Ma, B. Stenger, W. Liu, and H. Li, "Deblurring by realistic blurring," in *Proceedings of the IEEE Conference on Computer Vision and Pattern Recognition*, 2020, pp. 2737–2746.
- [51] S.-J. Chen and H.-L. Shen, "Multispectral image out-of-focus deblurring using interchannel correlation," *IEEE Transactions on Image Processing*, vol. 24, no. 11, pp. 4433–4445, 2015.
- [52] T. Hoßfeld, P. E. Heegaard, M. Varela, and S. Möller, "Qoe beyond the mos: an in-depth look at qoe via better metrics and their relation to mos," *Quality and User Experience*, vol. 1, no. 1, pp. 1–23, 2016.
- [53] A. Hore and D. Ziou, "Image quality metrics: Psnr vs. ssim," in *Proceedings of International Conference on Pattern Recognition*, 2010, pp. 2366–2369.
- [54] Z. Wang, A. C. Bovik, H. R. Sheikh, and E. P. Simoncelli, "Image quality assessment: from error visibility to structural similarity," *IEEE Transactions on Image Processing*, vol. 13, no. 4, pp. 600–612, 2004.
- [55] Z. Wang, E. P. Simoncelli, and A. C. Bovik, "Multiscale structural similarity for image quality assessment," in *Proceedings of Asilomar Conference on Signals, Systems & Computers*, 2003, pp. 1398–1402.
- [56] M. Heusel, H. Ramsauer, T. Unterthiner, B. Nessler, and S. Hochreiter, "Gans trained by a two time-scale update rule converge to a local nash equilibrium," in *Proceedings of Advances in Neural Information Processing Systems*, 2017.
- [57] R. Zhang, P. Isola, A. A. Efros, E. Shechtman, and O. Wang, "The unreasonable effectiveness of deep features as a perceptual metric," in *Proceedings of the IEEE Conference on Computer Vision and Pattern Recognition*, 2018, pp. 586–595.

- [58] A. K. Moorthy and A. C. Bovik, "A two-step framework for constructing blind image quality indices," *IEEE Signal Processing Letters*, vol. 17, no. 5, pp. 513–516, 2010.
- [59] M. A. Saad, A. C. Bovik, and C. Charrier, "Blind image quality assessment: A natural scene statistics approach in the dct domain," *IEEE Transactions on Image Processing*, vol. 21, no. 8, pp. 3339–3352, 2012.
- [60] A. Mittal, A. K. Moorthy, and A. C. Bovik, "No-reference image quality assessment in the spatial domain," *IEEE Transactions on Image Processing*, vol. 21, no. 12, pp. 4695–4708, 2012.
- [61] P. Ye, J. Kumar, L. Kang, and D. Doermann, "Unsupervised feature learning framework for no-reference image quality assessment," in *Proceedings of the IEEE Conference on Computer Vision and Pattern Recognition*, 2012, pp. 1098–1105.
- [62] A. K. Moorthy and A. C. Bovik, "Blind image quality assessment: From natural scene statistics to perceptual quality," *IEEE Transactions on Image Processing*, vol. 20, no. 12, pp. 3350–3364, 2011.
- [63] A. Mittal, R. Soundararajan, and A. C. Bovik, "Making a "completely blind" image quality analyzer," *IEEE Signal Processing Letters*, vol. 20, no. 3, pp. 209–212, 2012.
- [64] L. Liu, B. Liu, H. Huang, and A. C. Bovik, "No-reference image quality assessment based on spatial and spectral entropies," *Signal Processing: Image Communication*, vol. 29, no. 8, pp. 856–863, 2014.
- [65] P. Zhang, K. Zhang, W. Luo, C. Li, and G. Wang, "Blind face restoration: Benchmark datasets and a baseline model," *arXiv preprint arXiv:2206.03697*, 2022.
- [66] Y. Zhao, Y.-C. Su, C.-T. Chu, Y. Li, M. Renn, Y. Zhu, C. Chen, and X. Jia, "Rethinking deep face restoration," in *Proceedings of the IEEE Conference on Computer Vision and Pattern Recognition*, 2022, pp. 7652–7661.
- [67] Z. Liu, P. Luo, X. Wang, and X. Tang, "Deep learning face attributes in the wild," in *Proceedings of the IEEE International Conference on Computer Vision*, 2015, pp. 3730–3738.
- [68] X. Tu, J. Zhao, Q. Liu, W. Ai, G. Guo, Z. Li, W. Liu, and J. Feng, "Joint face image restoration and frontalization for recognition," *IEEE Transactions on Circuits and Systems for Video Technology*, vol. 32, no. 3, pp. 1285–1298, 2021.
- [69] J. Deng, J. Guo, E. Verferas, I. Kotsia, and S. Zafeiriou, "Retinaface: Single-shot multi-level face localisation in the wild," in *Proceedings of the IEEE Conference on Computer Vision and Pattern Recognition*, 2020, pp. 5203–5212.
- [70] N. Kumar, A. C. Berg, P. N. Belhumeur, and S. K. Nayar, "Attribute and simile classifiers for face verification," in *Proceedings of the IEEE International Conference on Computer Vision*, 2009, pp. 365–372.
- [71] J. Liu, R. Chen, S. An, and H. Zhang, "Cg-gan: Class-attribute guided generative adversarial network for old photo restoration," in *Proceedings of the ACM International Conference on Multimedia*, 2021, pp. 5391–5399.
- [72] W. Xia, Y. Yang, J.-H. Xue, and B. Wu, "Towards open-world text-guided face image generation and manipulation," *arXiv preprint arXiv:2104.08910*, 2021.
- [73] B. Dogan, S. Gu, and R. Timofte, "Exemplar guided face image super-resolution without facial landmarks," in *Proceedings of the IEEE Conference on Computer Vision and Pattern Recognition Workshops*, 2019.
- [74] K. Zhang, Z. Zhang, C.-W. Cheng, W. H. Hsu, Y. Qiao, W. Liu, and T. Zhang, "Super-identity convolutional neural network for face hallucination," in *Proceedings of the European Conference on Computer Vision*, 2018, pp. 183–198.
- [75] K. Grm, W. J. Scheirer, and V. Štruc, "Face hallucination using cascaded super-resolution and identity priors," *IEEE Transactions on Image Processing*, vol. 29, pp. 2150–2165, 2019.
- [76] J. Chen, J. Chen, Z. Wang, C. Liang, and C.-W. Lin, "Identity-aware face super-resolution for low-resolution face recognition," *IEEE Signal Processing Letters*, vol. 27, pp. 645–649, 2020.
- [77] D. Kim, M. Kim, G. Kwon, and D.-S. Kim, "Progressive face super-resolution via attention to facial landmark," in *Proceedings of British Machine Vision Conference*, 2019.
- [78] C. Chen, X. Li, L. Yang, X. Lin, L. Zhang, and K.-Y. K. Wong, "Progressive semantic-aware style transformation for blind face restoration," in *Proceedings of the IEEE Conference on Computer Vision and Pattern Recognition*, 2021, pp. 11 896–11 905.
- [79] X. Hu, W. Ren, J. Yang, X. Cao, D. P. Wipf, B. Menze, X. Tong, and H. Zha, "Face restoration via plug-and-play 3d facial priors," *IEEE Transactions on Pattern Analysis and Machine Intelligence*, 2021.
- [80] T. Karras, S. Laine, and T. Aila, "A style-based generator architecture for generative adversarial networks," in *Proceedings of the IEEE Conference on Computer Vision and Pattern Recognition*, 2019, pp. 4401–4410.
- [81] V. Le, J. Brandt, Z. Lin, L. Bourdev, and T. S. Huang, "Interactive facial feature localization," in *Proceedings of the European Conference on Computer Vision*, 2012, pp. 679–692.
- [82] X. Dong, Y. Yan, W. Ouyang, and Y. Yang, "Style aggregated network for facial landmark detection," in *Proceedings of the IEEE Conference on Computer Vision and Pattern Recognition*, 2018, pp. 379–388.
- [83] Y. Wu, T. Hassner, K. Kim, G. Medioni, and P. Natarajan, "Facial landmark detection with tweaked convolutional neural networks," *IEEE Transactions on Pattern Analysis and Machine Intelligence*, vol. 40, no. 12, pp. 3067–3074, 2017.
- [84] Q. Cao, L. Lin, Y. Shi, X. Liang, and G. Li, "Attention-aware face hallucination via deep reinforcement learning," in *Proceedings of the IEEE Conference on Computer Vision and Pattern Recognition*, 2017, pp. 690–698.
- [85] A. Bulat and G. Tzimiropoulos, "Super-fan: Integrated facial landmark localization and super-resolution of real-world low resolution faces in arbitrary poses with gans," in *Proceedings of the IEEE Conference on Computer Vision and Pattern Recognition*, 2018, pp. 109–117.
- [86] R. Kalarot, T. Li, and F. Porikli, "Component attention guided face super-resolution network: Cagface," in *Proceedings of the IEEE Winter Conference on Applications of Computer Vision*, 2020, pp. 370–380.
- [87] J. Kim, G. Li, C. Jung, and J. Kim, "Progressive face super-resolution with non-parametric facial prior enhancement," in *Proceedings of the IEEE International Conference on Image Processing*, 2021, pp. 899–903.
- [88] Y. Yu, P. Zhang, K. Zhang, W. Luo, C. Li, Y. Yuan, and G. Wang, "Multi-prior learning via neural architecture search for blind face restoration," *arXiv preprint arXiv:2206.13962*, 2022.
- [89] S. Zhu, S. Liu, C. C. Loy, and X. Tang, "Deep cascaded bi-network for face hallucination," in *Proceedings of the European Conference on Computer Vision*, 2016, pp. 614–630.
- [90] V. Chudasama, K. Nighania, K. Upla, K. Raja, R. Ramachandra, and C. Busch, "E-comsupsnet: Enhanced face super-resolution through compact network," *IEEE Transactions on Biometrics, Behavior, and Identity Science*, vol. 3, no. 2, pp. 166–179, 2021.
- [91] T. Lu, Y. Wang, Y. Zhang, Y. Wang, L. Wei, Z. Wang, and J. Jiang, "Face hallucination via split-attention in split-attention network," in *Proceedings of the ACM International Conference on Multimedia*, 2021, pp. 5501–5509.
- [92] K. Jiang, Z. Wang, P. Yi, T. Lu, J. Jiang, and Z. Xiong, "Dual-path deep fusion network for face image hallucination," *IEEE Transactions on Neural Networks and Learning Systems*, 2020.
- [93] Y. Gu, X. Wang, L. Xie, C. Dong, G. Li, Y. Shan, and M.-M. Cheng, "Vqfr: Blind face restoration with vector-quantized dictionary and parallel decoder," *arXiv preprint arXiv:2205.06803*, 2022.
- [94] X. Xu, D. Sun, J. Pan, Y. Zhang, H. Pfister, and M.-H. Yang, "Learning to super-resolve blurry face and text images," in *Proceedings of the IEEE International Conference on Computer Vision*, 2017, pp. 251–260.
- [95] X. Yu and F. Porikli, "Face hallucination with tiny unaligned images by transformative discriminative neural networks," in *Proceedings of the AAAI Conference on Artificial Intelligence*, vol. 31, no. 1, 2017.
- [96] A. Bulat, J. Yang, and G. Tzimiropoulos, "To learn image super-resolution, use a gan to learn how to do image degradation first," in *Proceedings of the European Conference on Computer Vision*, 2018, pp. 185–200.
- [97] W.-Z. Shao, J.-J. Xu, L. Chen, Q. Ge, L.-Q. Wang, B.-K. Bao, and H.-B. Li, "On potentials of regularized wasserstein generative adversarial networks for realistic hallucination of tiny faces," *Neurocomputing*, vol. 364, pp. 1–15, 2019.
- [98] F. Shiri, X. Yu, F. Porikli, R. Hartley, and P. Koniusz, "Identity-preserving face recovery from stylized portraits," *International Journal of Computer Vision*, vol. 127, no. 6, pp. 863–883, 2019.
- [99] T. Yang, P. Ren, X. Xie, and L. Zhang, "Gan prior embedded network for blind face restoration in the wild," in *Proceedings of the IEEE Conference on Computer Vision and Pattern Recognition*, 2021, pp. 672–681.
- [100] F. Zhu, J. Zhu, W. Chu, X. Zhang, X. Ji, C. Wang, and Y. Tai, "Blind face restoration via integrating face shape and generative priors," in *Proceedings of the IEEE Conference on Computer Vision and Pattern Recognition*, 2022, pp. 7662–7671.
- [101] A. Li, G. Li, L. Sun, and X. Wang, "Faceformer: Scale-aware blind face restoration with transformers," *arXiv preprint arXiv:2207.09790*, 2022.
- [102] S. Zhou, K. C. Chan, C. Li, and C. C. Loy, "Towards robust blind face restoration with codebook lookup transformer," *arXiv preprint arXiv:2206.11253*, 2022.

- [103] T. Karras, S. Laine, M. Aittala, J. Hellsten, J. Lehtinen, and T. Aila, "Analyzing and improving the image quality of stylegan," in *Proceedings of the IEEE Conference on Computer Vision and Pattern Recognition*, 2020, pp. 8110–8119.
- [104] I. Goodfellow, J. Pouget-Abadie, M. Mirza, B. Xu, D. Warde-Farley, S. Ozair, A. Courville, and Y. Bengio, "Generative adversarial nets," in *Proceedings of Advances in Neural Information Processing Systems*, 2014, p. 2672–2680.
- [105] A. Creswell, T. White, V. Dumoulin, K. Arulkumaran, B. Sengupta, and A. A. Bharath, "Generative adversarial networks: An overview," *IEEE Signal Processing Magazine*, vol. 35, no. 1, pp. 53–65, 2018.
- [106] V. Mnih, N. Heess, A. Graves *et al.*, "Recurrent models of visual attention," in *Proceedings of Advances in Neural Information Processing Systems*, 2014.
- [107] J. Hu, L. Shen, and G. Sun, "Squeeze-and-excitation networks," in *Proceedings of the IEEE Conference on Computer Vision and Pattern Recognition*, 2018, pp. 7132–7141.
- [108] C. Chen, D. Gong, H. Wang, Z. Li, and K.-Y. K. Wong, "Learning spatial attention for face super-resolution," *IEEE Transactions on Image Processing*, vol. 30, pp. 1219–1231, 2020.
- [109] Y. Wang, T. Lu, R. Xu, and Y. Zhang, "Face super-resolution by learning multi-view texture compensation," in *Proceedings of International Conference on Multimedia Modeling*, 2020, pp. 350–360.
- [110] T. Zhao and C. Zhang, "Saan: Semantic attention adaptation network for face super-resolution," in *Proceedings of IEEE International Conference on Multimedia and Expo*, 2020, pp. 1–6.
- [111] Z. Shen, W.-S. Lai, T. Xu, J. Kautz, and M.-H. Yang, "Deep semantic face deblurring," in *Proceedings of the IEEE Conference on Computer Vision and Pattern Recognition*, 2018, pp. 8260–8269.
- [112] Y. Yin, J. Robinson, Y. Zhang, and Y. Fu, "Joint super-resolution and alignment of tiny faces," in *Proceedings of the AAAI Conference on Artificial Intelligence*, vol. 34, no. 07, 2020, pp. 12 693–12 700.
- [113] K. Li, B. Bare, B. Yan, B. Feng, and C. Yao, "Face hallucination based on key parts enhancement," in *Proceedings of the IEEE International Conference on Acoustics, Speech and Signal Processing*, 2018, pp. 1378–1382.
- [114] M. Li, Z. Zhang, J. Yu, and C. W. Chen, "Learning face image super-resolution through facial semantic attribute transformation and self-attentive structure enhancement," *IEEE Transactions on Multimedia*, vol. 23, pp. 468–483, 2020.
- [115] C. Ma, Z. Jiang, Y. Rao, J. Lu, and J. Zhou, "Deep face super-resolution with iterative collaboration between attentive recovery and landmark estimation," in *Proceedings of the IEEE Conference on Computer Vision and Pattern Recognition*, 2020, pp. 5569–5578.
- [116] A. Dosovitskiy, L. Beyer, A. Kolesnikov, D. Weissenborn, X. Zhai, T. Unterthiner, M. Dehghani, M. Minderer, G. Heigold, S. Gelly *et al.*, "An image is worth 16x16 words: Transformers for image recognition at scale," in *Proceedings of International Conference on Learning Representation*, 2021.
- [117] A. Vaswani, N. Shazeer, N. Parmar, J. Uszkoreit, L. Jones, A. N. Gomez, Ł. Kaiser, and I. Polosukhin, "Attention is all you need," in *Proceedings of Advances in Neural Information Processing Systems*, 2017.
- [118] N. Carion, F. Massa, G. Synnaeve, N. Usunier, A. Kirillov, and S. Zagoruyko, "End-to-end object detection with transformers," in *Proceedings of the European Conference on Computer Vision*, 2020, pp. 213–229.
- [119] W. Wang, E. Xie, X. Li, D.-P. Fan, K. Song, D. Liang, T. Lu, P. Luo, and L. Shao, "Pyramid vision transformer: A versatile backbone for dense prediction without convolutions," in *Proceedings of the IEEE International Conference on Computer Vision*, 2021, pp. 568–578.
- [120] Z. Liu, Y. Lin, Y. Cao, H. Hu, Y. Wei, Z. Zhang, S. Lin, and B. Guo, "Swin transformer: Hierarchical vision transformer using shifted windows," in *Proceedings of the IEEE International Conference on Computer Vision*, 2021, pp. 10 012–10 022.
- [121] K. He, X. Zhang, S. Ren, and J. Sun, "Deep residual learning for image recognition," in *Proceedings of the IEEE Conference on Computer Vision and Pattern Recognition*, 2016, pp. 770–778.
- [122] Y. Tai, J. Yang, and X. Liu, "Image super-resolution via deep recursive residual network," in *Proceedings of the IEEE Conference on Computer Vision and Pattern Recognition*, 2017, pp. 3147–3155.
- [123] G. Huang, Z. Liu, L. Van Der Maaten, and K. Q. Weinberger, "Densely connected convolutional networks," in *Proceedings of the IEEE Conference on Computer Vision and Pattern Recognition*, 2017, pp. 4700–4708.
- [124] Y. Liu, Z. Dong, K. P. Lim, and N. Ling, "A densely connected face super-resolution network based on attention mechanism," in *Proceedings of IEEE Conference on Industrial Electronics and Applications*, 2020, pp. 148–152.
- [125] K. Simonyan and A. Zisserman, "Very deep convolutional networks for large-scale image recognition," in *Proceedings of International Conference on Learning Representation*, 2014.
- [126] O. Jesorsky, K. J. Kirchberg, and R. W. Frischholz, "Robust face detection using the hausdorff distance," in *Proceedings of International Conference on Audio-and Video-based Biometric Person Authentication*, 2001, pp. 90–95.
- [127] G. B. Huang, M. Mattar, T. Berg, and E. Learned-Miller, "Labeled faces in the wild: A database for studying face recognition in unconstrained environments," in *Proceedings of Workshop on Faces in Real-Life Images: Detection, Alignment, and Recognition*, 2008.
- [128] M. Koestinger, P. Wohlhart, P. M. Roth, and H. Bischof, "Annotated facial landmarks in the wild: A large-scale, real-world database for facial landmark localization," in *Proceedings of the IEEE International Conference on Computer Vision Workshops*, 2011, pp. 2144–2151.
- [129] C. Sagonas, G. Tzimiropoulos, S. Zafeiriou, and M. Pantic, "300 faces in-the-wild challenge: The first facial landmark localization challenge," in *Proceedings of the IEEE International Conference on Computer Vision Workshops*, 2013, pp. 397–403.
- [130] X. Zhu, Z. Lei, X. Liu, H. Shi, and S. Z. Li, "Face alignment across large poses: A 3d solution," in *Proceedings of the IEEE Conference on Computer Vision and Pattern Recognition*, 2016, pp. 146–155.
- [131] A. Bulat and G. Tzimiropoulos, "How far are we from solving the 2d & 3d face alignment problem?(and a dataset of 230,000 3d facial landmarks)," in *Proceedings of the IEEE International Conference on Computer Vision*, 2017, pp. 1021–1030.
- [132] D. Yi, Z. Lei, S. Liao, and S. Z. Li, "Learning face representation from scratch," *Computer Science*, 2014.
- [133] R. Rothe, R. Timofte, and L. Van Gool, "Dex: Deep expectation of apparent age from a single image," in *Proceedings of the IEEE International Conference on Computer Vision Workshops*, 2015, pp. 10–15.
- [134] O. M. Parkhi, A. Vedaldi, and A. Zisserman, "Deep face recognition," in *Proceedings of British Machine Vision Conference*, 2015.
- [135] S. Zafeiriou, G. Trigeorgis, G. Chrysos, J. Deng, and J. Shen, "The menpo facial landmark localisation challenge: A step towards the solution," in *Proceedings of the IEEE Conference on Computer Vision and Pattern Recognition Workshops*, 2017, pp. 170–179.
- [136] Q. Cao, L. Shen, W. Xie, O. M. Parkhi, and A. Zisserman, "Vggface2: A dataset for recognising faces across pose and age," in *Proceedings of the IEEE International Conference on Automatic Face & Gesture Recognition*, 2018, pp. 67–74.
- [137] J. Deng, J. Guo, N. Xue, and S. Zafeiriou, "Arcface: Additive angular margin loss for deep face recognition," in *Proceedings of the IEEE Conference on Computer Vision and Pattern Recognition*, 2019, pp. 4690–4699.
- [138] Y. Sun, Y. Chen, X. Wang, and X. Tang, "Deep learning face representation by joint identification-verification," in *Proceedings of Advances in Neural Information Processing Systems*, 2014.
- [139] K. Zhang, Z. Zhang, Z. Li, and Y. Qiao, "Joint face detection and alignment using multitask cascaded convolutional networks," *IEEE Signal Processing Letters*, vol. 23, no. 10, pp. 1499–1503, 2016.
- [140] A. Shafaei, J. J. Little, and M. Schmidt, "Autoretouch: Automatic professional face retouching," in *Proceedings of the IEEE Winter Conference on Applications of Computer Vision*, 2021, pp. 990–998.
- [141] M. Zhu, C. Liang, N. Wang, X. Wang, Z. Li, and X. Gao, "A sketch-transformer network for face photo-sketch synthesis," in *Proceedings of International Joint Conference on Artificial Intelligence*, 2021, pp. 1352–1358.
- [142] P. KR, R. Mukhopadhyay, J. Philip, A. Jha, V. Nambodiri, and C. Jawahar, "Towards automatic face-to-face translation," in *Proceedings of the ACM International Conference on Multimedia*, 2019, pp. 1428–1436.
- [143] Z. Wan, B. Zhang, D. Chen, P. Zhang, D. Chen, J. Liao, and F. Wen, "Bringing old photos back to life," in *Proceedings of the IEEE Conference on Computer Vision and Pattern Recognition*, 2020, pp. 2747–2757.